to cells or virus-infected cells to uninfected cells. Moscona et al. demonstrated that desialylated cells are unable to fuse with parainfluenza virus-infected cells [23]. Another sialic acid-related fusion mechanism occurs in sperm–egg fusion. Egg surface sialic acid has a role in triggering the sperm acrosome reaction, an exocytotic event required for membrane fusion of the gametes in sperm–egg fusion [9]. To our knowledge, however, there are no reports of the involvement of cell surface sialic acid in osteoclast fusion.

Sialic acid is also called neuraminic acid, which represents a family of derivatives of C9 sugar that include carboxylic acid, and are components of glycoproteins and glycolipids. In mouse, there are mainly two kinds of sialic acid, *N*-acetylneuraminic acid and *N*-glycolylneuraminic acid. Humans have only *N*-acetylneuraminic acid. Sialylated glycoconjugates are present on many mammalian cell membranes and are implicated in many biologic processes, such as intercellular adhesive reactions, hematopoietic cell differentiation, and virus–cell fusion [4,14,29,31]. The structural diversity, peripheral position of sialic acid on oligosaccharide chains of glycoconjugates, and regulated expression of sialylglycoconjugates appear to correlate with their functions [36]. The surfaces of monocyte/macrophage lineage cells contain sialylated glycoproteins and glycolipids and the functional capacity of these cells changes after the removal of sialic acid from the cell surface glycoconjugates [29]. Because osteoclasts are of the monocyte/macrophage lineage and a lectin-histochemical study of pathologic bone tissue demonstrated the membranous and intracytoplasmic distribution of sialic acids in osteoclasts and osteoclast precursor cells [10], we hypothesized that the sialic acid of cell surface glycoconjugates is involved in osteoclast fusion.

In the present study, we first investigated the change in glycoconjugate sialylation during osteoclast differentiation, and then examined the effect of desialylation of osteoclast precursors on the differentiation of osteoclasts, especially in the cell–cell fusion process.

Materials and methods

Animals and reagents

Male ddY mice (6–9 weeks old) were purchased from Sankyo Laboratories (Tokyo, Japan). The studies using mice were approved by the institutional animal review board. Recombinant human macrophage-colony stimulating factor (rhM-CSF) was purchased from Wako Pure Chemical Industry Co., Ltd. (Osaka, Japan). Soluble recombinant human receptor activator of nuclear factor-κB ligand (sRANKL) was purchased from PeproTech EC, Ltd. (London, U.K.). Sialidase (SAase; provided as neuraminidase from Arthrobacter Ureafaciens) was purchased from Nacalai Tesque, Inc. (Kyoto, Japan). Fluorescein isothiocyanate (FITC)-labeled lectin Arachis hypogaea (PNA), Maackia amurensis (MAA), and Sambucus nigra (SNA-I) were purchased from EY Laboratories (San Mateo, CA). All the antibodies used in this study were purchased from Cell Signaling (Beverly, MA).

Osteoclastogenesis assay

Osteoclast differentiation from bone marrow cells was achieved as previously described with slight modification [34]. Briefly, femurs and tibias of adult mice were aseptically removed and dissected free of adhering tissues. The bone ends were cut off with scissors and the marrow cavity was flushed with α-minimum essential medium (α-MEM). The marrow cells were collected, washed with α-MEM, and red blood cells were removed by treatment with 0.727% NH4Cl-0.017% Tris–Cl (pH7.2)-phosphate-buffered saline (PBS) solution. After washing, cells were cultured in α-MEM containing 10% fetal bovine serum (FBS), 100 IU/ml penicillin G (Meiji Seika, Tokyo, Japan), 100 μg/ml streptomycin (Meiji Seika), and rhM-CSF (30 ng/ml) at 5×10^6 cells in a 10-cm suspension culture dish (Corning Costar Inc., Corning, NY). After 3-day culture, cells were washed vigorously with PBS twice to remove nonadherent cells and bone marrow macrophage cells (BMMs) were harvested by pipetting with 0.02% EDTA in PBS. BMMs were resuspended in the α-MEM containing 10% FBS, 30 ng/ml rhM-CSF, and 100 ng/ml sRANKL, and cultured on 48-well plates (1×10^5 cells/well). Cells were incubated for 3 days at 37 °C in a 5% humidified CO_2 incubator.

The osteoclastogenic differentiation of the murine monocyte/macrophage cell line RAW264.7 was achieved by seeding the cells at a density of 1×10^4 cells/well in 48-well plates and culturing for 5 days with 50 ng/ml sRANKL in Dulbecco's MEM (DMEM) containing 10% FBS.

Lectin histochemical analysis

Cells were cultured on glass coverslips and fixed for 5 min with 4% paraformaldehyde and then treated with 0.1% Triton X-100 to permeate the cell membrane. After blocking with 1% bovine serum albumin, cells were incubated with FITC-labeled MAA lectin or FITC-labeled SNA-I lectin, and reacted with 4′,6-diamidino-2-phenylindole, dihydrochloride (Dojindo Laboratories, Japan), and phalloidin-tetramethyl isothiocyanate (Sigma Chemical Co., St. Louis, MO, P1951) to identify nuclei and F-actin. MAA binds to alpha (2,3)-linked-sialic acid and SNA-I binds to alpha (2,6)-linked-sialic acid, respectively. Cells were then mounted on glass slides and examined with a confocal laser-scanning microscope (Fluoview FV300, Olympus).

Treatment of osteoclast precursor cells with exogenous SAase

To evaluate the role of cell surface sialic acid in the osteoclast differentiation process, cell surface glycoconjugates were desialylated by exogenous SAase. In an osteoclastogenesis assay, cells were exposed to either SAase (100 mU/ml, 10 mU/ml, 1 mU/ml, or 0 mU/ml) or heat-inactivated SAase (100 mU/ml).

Removal of sialic acid from the plasma membrane was ascertained as described by Stamatos et al. [29]. Cells were desialylated with 100 mU/ml SAase for 3 h in a moist chamber, and then treated with FITC-labeled lectin PNA and analyzed by fluorescent microscopy and flow cytometry. PNA binds to the galactose moiety that is exposed on cell surface glycoconjugates after removal of the terminal sialic acid. For flow-cytometry, mock- and SAase-treated cells (2×10^5) were suspended in 0.1 ml PBS, pH 7.4, containing 2% FBS, and incubated with 10 μg/ml FITC-labeled PNA or left unstained. Cells were incubated with PNA for 45 min at 4 °C before unbound lectin was removed by washing the cells at 4 °C with 2 ml PBS, pH 7.4, containing 2% bovine serum albumin. Cells were fixed in 1% paraformaldehyde and analyzed by flow cytometry using a Becton Dickinson FACS Caliber (Becton Dickinson, Franklin Lakes, NJ). Data were analyzed using CELL Quest data analysis software (Becton Dickinson).

Kinetics of sialic acid expression on plasma membranes during osteoclastogenesis

To analyze the kinetics of sialic acid expression on plasma membranes during osteoclastogenesis with or without SAase treatment, we quantitatively investigated the alpha (2,3)-linked-sialic acid and alpha (2,6)-linked-sialic acid content by flow cytometry. We prepared four different conditioned RAW 264.7 cells cultured with DMEM and 10% FBS: (1) no treatment, (2) desialylated with 100 mU/ml SAase for 3 h, (3) cultured with sRANKL (50 ng/ml) for 4 days, and (4) desialylated with 100 mU/ml SAase and cultured with sRANKL (50 ng/ml) for 4 days. These cells were treated with FITC-labeled lectin MAA (50 μg/ml) or FITC-labeled lectin SNA-I (50 μg/ml) and analyzed by flow cytometry as described above.

Tartrate-resistant acid phosphatase (TRAP) staining and TRAP activity measurement

Osteoclast generation was confirmed by TRAP staining. After aspiration of medium, cells were fixed with 1% glutaraldehyde in PBS for 5 min at room temperature and stained for TRAP using a histochemical kit (Hokudo, Co, Ltd. Japan) according to the manufacturer's instructions. Mature osteoclasts were identified microscopically as TRAP-positive cells with at least three nuclei and the number of cells was quantified for each well.

TRAP activity of the cell culture supernatant was measured using a TRAP activity assay kit according to the manufacturer's protocol (Hokudo, Co, Ltd.). Briefly, 30 μl of cell culture supernatant was retrieved and mixed with TRAP staining solution in 96-well plates. The plates were incubated in a moist chamber at 37 °C for 3 h and the absorbance of the solution was measured at 540 nm.

Resorption pit assay

Osteoclasts were further characterized by assessing their ability to form resorption pits on dentin slices. Dentin slices were purchased from Hokudo, Co., Ltd. The slices were placed in 48-well plates and BMM cells were seeded into each well with α-MEM containing 10% FBS, 30 ng/ml rhM-CSF, and 100 ng/ml sRANKL. After 10-day culture with or without SAase treatment, dentin slices were sonicated in 1 M ammonia solution to remove the cells and stained with hematoxylin. The area of resorption lacunae (pits) on each slice was measured and analyzed with Image J software (http://rsb.info.nih.gov/nih-image/).

Real-time polymerase chain reaction (PCR) quantification of gene expression

Total RNA from cultured cells was isolated using the Qiagen RNeasy Mini Kit according to the manufacturer's instructions (Qiagen, Valencia, CA). cDNA were synthesized from 1 μg total RNA using reverse transcriptase and oligo-dT primers in a volume of 10 μl, and the reaction mixture was adjusted to 50 μl with TE buffer (10 mM Tris–1 mM EDTA, pH 8.0) for PCR analysis. PCR was performed and monitored using the DNA Engine Opticon 2 System (MJ Research, Hercules, CA). The 2× SYBR Green Mastermix (DyNAmo™ HS SYBR Green qPCR Kit) was based on a hot start version of a modified Thermus brockianus DNA polymerase (Finnzymes Oy, Finland). cDNA samples (5 μl for a total volume of 20 μl per reaction) were analyzed for both the genes of interest and the reference genes (glyceraldehyde-3-phosphate dehydrogenase; GAPDH). Primer sequences used for mouse beta galactoside alpha (2,3) sialyltransferase-I, -II, -III, -IV, V (ST3Gal-I, II, III, IV, V), and beta galactoside alpha (2,6) sialyltransferase-I, -II (ST6Gal-I, -II), calcitonin receptor, cathepsin K, integrin β3, nuclear factor of activated T cells c1 (NF-ATc1), and GAPDH are shown in Table 1. Cycle threshold (Ct) values were obtained graphically. Relative expression was calculated using the comparative Ct method. Samples were normalized for the expression of GAPDH by calculating the ΔCt (Ct gene of interest − Ct GAPDH); subsequently, the ΔΔCt values were calculated by ΔCt sample − ΔCt calibrator, where the calibrator is the control sample (unstimulated BMMs). Relative expression of the different genes is expressed as $2-(\Delta Ct)$.

Small interfering RNA (SiRNA)

Three duplexed Stealth™ siRNAs designed against the ST6Gal-I (accession no. NM_145933) were purchased from Invitrogen (Carlsbad, CA): MSS237905, sense 5′-AUAAUGAUGAUACCCAGCAUGCCGG-3′, antisense 5′-CCGGCAUGCUGGGUAUCAUCAUUAU-3′; MSS237906, sense 5′-UUAUCAAUCUCUCGACCCAGCUGGG-3′, antisense 5′-CCCAGCUGGGUCGAGAGAUUGAUAA-3′; MS237907, sense 5′-AAGACACGACGGCACACUUAUGCCA-3′, antisense 5′-UGGCAUAAGUGUGCCGUCGUGUCUU-3′. Transfection efficacy was analyzed using 50 nM BLOCK-iT™ Alexa Fluor® Red Fluorescent Oligo (Invitrogen). Preliminary experiments indicated that siRNA MS237907 most efficiently downregulated the ST3Gal-I mRNA expression in RANKL-stimulated RAW 264.7 cells.

To investigate the role of ST6Gal-I in osteoclast differentiation, RANKL-stimulated RAW 264.7 cells in 48-well plates were transfected using either 50 nM siRNA control (Stealth RNAi negative control, Invitrogen) or siRNA MS209002 combined with 0.8 μl Lipofectamine RNAiMax (Invitrogen) in Opti-MEM media supplemented with sRANKL on day 1 of differentiation. Media were replaced every 2 days after RANKL stimulation by DMEM with 10% FBS and sRANKL. No antibiotics were used. The cells were incubated for 4 days (72 h after transfection) at 37 °C in a CO2 incubator, after which they were fixed in 1% glutaraldehyde in PBS. TRAP staining was performed to confirm the presence of TRAP-positive multinuclear cells (MNCs).

Statistical analysis

Results are shown as the mean ± SD of at least three experiments. Data were statistically analyzed using one factor analysis of variance followed by Bonferroni/Dunn test as a post hoc analysis for the osteoclast formation assay. For the bone resorption assay and siRNA knock down assay, statistical analysis was performed using Student's *t*-test. A P value of less than 0.05 was considered to be statistically significant.

Results

Expression of sialic acid in osteoclast precursor cells and osteoclasts

First, we confirmed the existence of alpha (2,3)-linked-sialic acid stained with MAA lectin and alpha (2,6)-linked-sialic acid stained with SNA-I lectin in osteoclast precursors by lectin histochemical study (Fig. 1). In BMMs, both alpha (2,3)-linked-sialic acid and alpha (2,6)-linked-sialic acid were distributed in the paranuclear area and cytoplasm. After 3-day culture in the

Table 1
Sequence of primers used in quantitative RT-PCR

Gene	Forward primers (5′–3′)	Reverse primers (5′–3′)	Amplicon (bp)	Accession number
ST3Gal-I	CCA ACA ACC TGA GCG ACA	TCC TAC AAC TGC ACA GCG TC	110	NM_009177
ST3Gal-II	AAG TGC TCT CTT CGG GTG TG	GCT GTG GTG CGA GTA GGT G	87	BC066064
ST3Gal-III	AGC CAC CAA GTA CGC AAA CT	CCT AGC CCA CTT GCG AAA G	136	NM_009176
ST3Gal-IV	CGA CGT GGT CAT CAG ATT GA	GGG CCG ACT CAG GAT AGA AG	98	NM_009178
ST3Gal-V	GTG GAC CCT GAC CGG ATA AA	CAT AGC CGT CTT CGC GTA CC	90	NM_011375
ST6Gal-I	CTG GGC CTT GGC ATA AGT G	AAA CCT CAG GAC CGC ATC AT	101	NM_145933
ST6Gal-II	GGA GAC ATC ATG GCG ATC A	CAT GTC GCT GTC ATA GGC TT	97	NM_172829
CTR	TGG CTG TGT TTA CCG ACG AG	CGA GTG ATG GCG TGG ATA AT	146	NM_007588
Cathepsin K	TGGATGAAATCTCTCGGCGT	TCATGTCTCCCAAGTGGTTC	123	NM_007802
Int ß3	TGACTCGGACTGGACTGGCTA	CACTCAGGCTCTTCCACCACA	414	NM_016780
NF-ATc1	CCT GGA GAT CCC GTT GC	GGT GTT CTT CCT CCC GAT GT	135	AF239169
GAPDH	ACTTTGTCAAGCTCATTTCC	TGCAGCGAACTTTATTGATG	269	BC098095

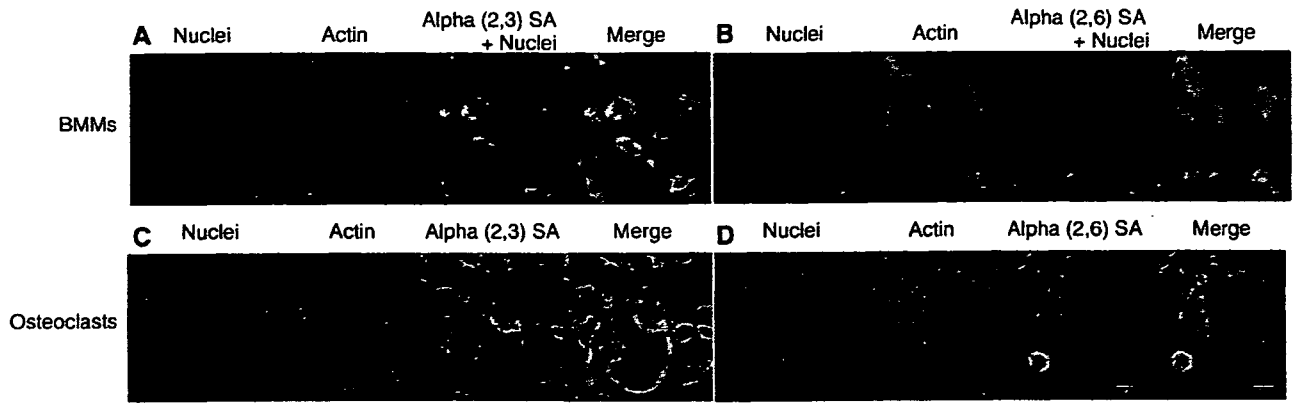

Fig. 1. Immunohistochemical study of the alpha (2,3)-linked sialic acid (alpha (2,3) SA) stained with MAA lectin and alpha (2,6)-linked-sialic acid (alpha (2,6)-SA) stained with SNA-I lectin in BMM and osteoclasts. Nuclei were stained with DAPI and actin was stained with phalloidin-TRITC. (A, C) Alpha (2,3)-SA is expressed in BMM, and after 3-day culture in the presence of rhM-CSF and sRANKL, alpha (2,3)-SA accumulated on the plasma membrane in pre-fusion mononuclear cells. Alpha (2,3)-SA is also expressed in the paranuclear area and the area consistent with the actin ring in polykaryocytes. (B, D) Alpha (2,6)-SA is expressed in BMMs, and accumulates on the cell surface of pre-fusion mononuclear cells, whereas it is markedly decreased in the cells in which cell fusion was complete with actin ring formation.

presence of rhM-CSF and sRANKL, mononuclear cells undergoing cell fusion accumulated both alpha (2,3)-linked-sialic acid and alpha (2,6)-linked-sialic acid on the plasma membrane. In multinuclear giant cells with actin ring formation, alpha (2,3)-linked-sialic acid was still expressed in the paranuclear area and along the actin ring, whereas the expression of alpha (2,6)-linked-sialic acid was degraded in polykaryocytes.

To gain insight into the mechanisms underlying changes in the expression of alpha (2,3)-linked and alpha (2,6)-linked sialic acids during osteoclastogenesis, we investigated the alterations in mRNA expression of the known cloned sialyltransferases (ST3Gal-I, II, III, IV, V, and ST6Gal-I, II) before and after RANKL stimulation (Fig. 2). Of those sialyltransferases, the results of real-time RT-PCR analysis showed that all five beta galactoside alpha (2,3)-sialyltransferases were expressed in BMMs, whereas only ST6Gal-I was expressed in two of the beta galactoside alpha (2,6)-sialyltransferases. mRNA expression of ST3Gal-I and ST3Gal-V changed significantly after RANKL stimulation.

Most of the potential sialylation sites of accessible glycoconjugates on the osteoclast precursor surface are sialylated

BMMs stimulated with rhM-CSF and sRANKL for 1 day were desialylated with exogenous SAase and removal of sialic acid from cell surface glycoconjugates was confirmed by PNA lectin staining that bound specifically to the exposed penultimate galactose residue of desialylated cell surface glycoconjugates (Figs. 3A–D). FITC-labeled PNA bound to the surface of mock-treated BMM, yielding a mean channel fluorescence of 18 (Fig. 3E, dotted line), which was approximately 4-fold greater than the fluorescence of unstained mock-treated cells (Fig. 3E, black area). After BMMs were treated with 100 mU/ml SAase for 3 h, there was a greater than 31-fold increase in the amount of PNA that bound to the cell surface (mean channel fluorescence, 123; Fig. 3E, gray area). Thus, at least 88% of potential sialylation sites on cell surface glycoconjugates that were accessible to exogenous SAase were sialylated in BMMs.

Desialylation of osteoclast precursor cells inhibits RANKL-induced MNC formation during osteoclastogenesis

SAase treatment inhibited rhM-CSF and RANKL-induced osteoclast differentiation from BMMs to TRAP-positive multinuclear osteoclasts in a dose-dependent manner (Figs. 4A–I). SAase concentrations of 10 mU/ml more significantly reduced the formation of multinuclear mature osteoclasts compared to mock-treated cells. Morphologically, BMMs that were spindle-shaped on the culture dish at Day 1 became small round mononuclear cells at Day 2. During this 2-day period, there was no apparent difference between mock-treated cells and SAase treated cells. After 3-day culture, TRAP-positive MNCs were formed in mock-treated and heat-inactivated SAase-treated cells, whereas there was a small number of TRAP-positive MNCs in SAase-treated cell cultures. In SAase-treated cell culture, there were TRAP-positive mononuclear cells. TRAP activity of the cell culture supernatant increased after rhM-CSF and sRANKL stimulation, and the TRAP activity value was significantly lower in SAase-treated cells compared to mock-treated cells (Fig. 4J).

To investigate the bone resorbing ability of osteoclasts differentiated from desialylated BMMs, the resorption pit areas of dentin slices were measured after 10-day culture with or without SAase treatment (Fig. 4L). The resorption pit area in 100 mU/ml SAase-treated cells was 8.7±2.9%, significantly smaller than the area of 42.9±7.9% in mock-treated cells. The resorption pit size was comparatively small with no continuity in 100 mU/ml SAase-treated cells.

A similar inhibitory effect of SAase treatment on osteoclast differentiation was observed in sRANKL-induced osteoclastogenesis of RAW 264.7 cells (Figs. 4M, N). The number of TRAP-positive MNCs in 100 mU/ml SAase-treated cells decreased significantly. There was no significant difference

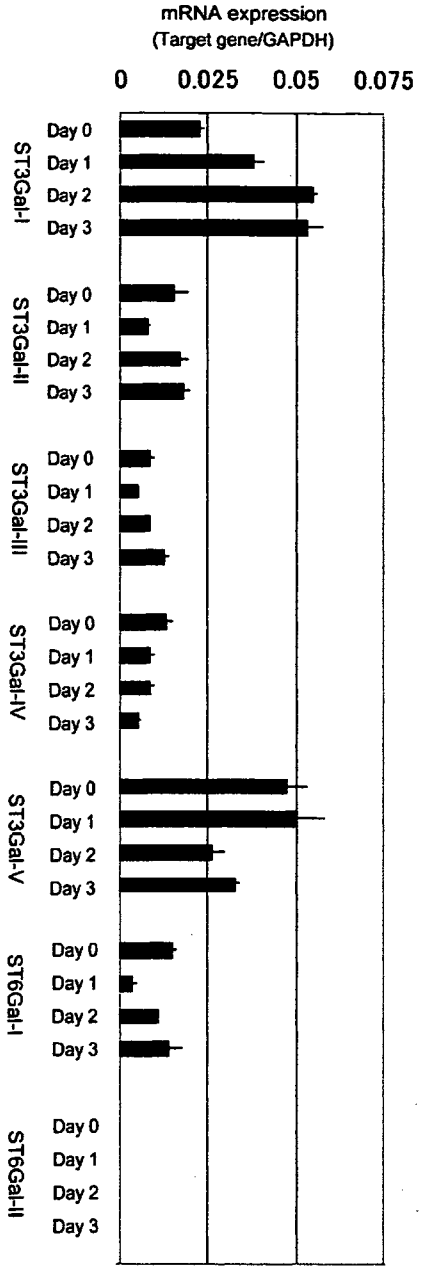

Fig. 2. Quantitative real-time RT-PCR analysis. mRNA expression of sialyltransferases during osteoclastogenesis. BMMs were cultured in the presence of rhM-CSF (30 ng/ml) and sRANKL (100 ng/ml). The mean and SD of three examinations are shown. ST3Gal-I, II, III, IV, V (mouse beta galactoside alpha 2,3 sialyltransferase-I, -II, -III, -IV, -V), and ST6Gal-I, -II (beta galactoside alpha 2,6 sialyltransferase-I, -II).

between mock-treated and 1 to 10-mU/ml SAase-treated cells in the number of TRAP-positive MNCs, but the size of the cells and the number of nuclei in the osteoclasts in the mock-treated group were obviously larger than those in the SAase-treated cells.

Effects of desialylation of cell surface glycoconjugates on osteoclast-related gene expression

To gain insight into the effect of desialylation of osteoclast precursor cells on osteoclast differentiation, mRNA expression levels of osteoclast-related genes induced during osteoclastogenesis were investigated by quantitative real-time RT-PCR (Fig. 4K). The calcitonin receptor, cathepsin K, integrin β3, and NF-ATc1 genes were induced during the first 2 day with a similar trend in both mock-treated and SAase-treated cells. SAase treatment blocked mRNA expression of the calcitonin receptor and NFATc1 at day 3, but did not affect the expression of cathepsin K and integrin β3 throughout the entire differentiation period.

Kinetics of sialic acid expression on plasma membranes during osteoclastogenesis

Flow cytometric analysis of surface lectin staining showed the change in cell surface sialic acid content during osteoclastogenesis (Fig. 5). Alpha (2,3)-linked sialic acid was highly expressed on the surface of these osteoclast precursor cells, and was still expressed at day 4 after sRANKL stimulation. Alpha (2,6)-linked-sialic acid was also detected in the osteoclast precursor cells, whereas its expression markedly decreased in half of the cells at day 4 after sRANKL stimulation (Fig. 5G). At day 4 after RANKL stimulation, there were cells in various stages, including pre-fusion osteoclasts and cells that had completed cell fusion. This means that only the alpha (2,6)-linked-sialic acid content was significantly reduced with osteoclast differentiation.

We also investigated the change in sialic acid content before and after SAase digestion (Figs. 5B, D, F, H). The exogenous SAase slightly changed the alpha (2,3)-linked-sialic acid content, whereas it effectively removed alpha (2,6)-linked-sialic acid. These findings indicate that SAase can easily access alpha (2,6)-linked-sialic acid, but cannot access alpha (2,3)-linked-sialic acid on the surface of osteoclast precursor cells.

Knockdown of ST6Gal-I with siRNA

Because the inhibitory effects of SAase treatment on osteoclast differentiation are considered to derive from the removal of alpha (2,6)-linked-sialic acid, we further characterized the role of alpha (2,6)-linked-sialic acid in osteoclast differentiation using ST6Gal-I knockdown cells. Preliminary studies showed that the mean transfection efficiency was 70% to 80% of the total cells at 48 h after transfection, based on the uptake of a fluorescent double-stranded oligomer. Among the three siRNAs against targets in ST6Gal-I, siRNA MS237907 most effectively downregulated ST6Gal-I mRNA expression (Fig. 6).

In the osteoclastogenesis assay, cells were transfected with MS237907 or control siRNAs at 1 day after sRANKL stimulation and examined 72 h after transfection. Cells transfected with control siRNA showed TRAP-positive multinuclear giant cell formation (Fig. 6B). In contrast, TRAP-positive multinuclear giant cells were rarely observed in ST6Gal-I knockdown cells.

Discussion

The results of the present study suggest that sialylation of cell surface glycoconjugates has an important role in osteoclast differentiation. Sialic acid is expressed in osteoclast precursors,

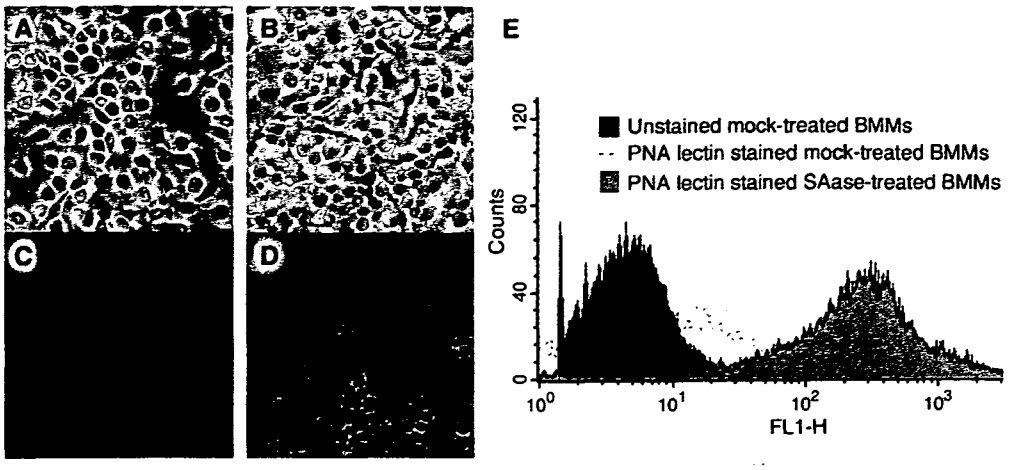

Fig. 3. PNA lectin staining of osteoclast precursor cells with or without SAase treatment. PNA binds to the galactose moiety that is exposed on cell surface glycoconjugates after the removal of the terminal sialic acid. (A, C) Mock-treated BMMs. (B, D) SAase-treated BMMs. (C, D) FITC-PNA lectin staining. (E) FACs analysis of BMMs.

and subsequently accumulates on the cell surface after RANKL stimulation. Interestingly, removal of sialic acid from cell surface glycoconjugates appeared to strongly inhibit osteoclast differentiation, suggesting that cell surface sialic acid is involved in osteoclast differentiation. Furthermore, the findings that desialylated osteoclast precursor cells formed TRAP-positive mononuclear cells, but MNC formation in both BMMs and RAW 264.7 cell lines was inhibited, indicate that sialic acid is involved in the osteoclast fusion process. Considering the fact that sialic acid is implicated in cell–cell adhesive reactions, especially in hematopoietic cells [4,27,8,13], both in ligand-promoting interactions in virus–cell fusion and in selectin-mediated cell–cell adhesion, it is reasonable to suppose that the sialic acid of osteoclast precursor cells mediates cell–cell fusion during osteoclast differentiation.

Among several structurally diverse sialylated glycoconjugates, the results of this study suggest that alpha (2,6) linked-sialic acid is probably the most important for osteoclast cell–cell fusion. As an interesting result of the sialic acid study, alpha (2,6)-linked-sialic acid, which is expressed on the surface of pre-fusion mononuclear cells, markedly decreased once the cells completed fusion to polykaryocytes, suggesting that alpha (2,6)-linked-sialic acid might be involved in the cell–cell fusion process. Because our flow cytometric analysis of surface lectin staining demonstrated that the exogenous SAase effectively removed alpha (2,6)-linked-sialic acid but only slightly changed the alpha (2,3)-linked-sialic acid content, the inhibitory effect of SAase treatment on osteoclast differentiation is considered to derive from the deficiency of alpha (2,6)-linked-sialic acid. The reason for the discrepancy in the efficacy of SAase to remove structurally diverse sialylated glycoconjugates might be that most of the alpha (2,6)-linked-sialic acid is accessible to the exogenous SAase, but alpha (2,3)-linked-sialic acid is not accessible to it because of the conformational structure of sialylglycoconjugates. Furthermore, the fact that ST6Gal-I knockdown cells markedly reduced the ability to form TRAP-positive MNC, supports the idea that alpha (2,6)-linked-sialic acid on the osteoclast precursor cells might be responsible for osteoclast maturation, possibly via its role in the cell–cell fusion process.

Although the mechanism by which sialic acid mediates osteoclast cell–cell fusion remains unclear, there are some candidate molecules or mechanisms based on previous studies of sialic acid. One is a lectin-associated protein such as the macrophage-restricted plasma membrane receptor known as sialoadhesin. Sialoadhesin is a prototypic member of the Siglec family of sialic acid binding immunoglobulin-like lectins that is expressed in subpopulations of macrophages, including bone marrow and inflammatory macrophages [27,8]; however, this molecule mediates cell–cell adhesion via recognition of a particular alpha (2,3)-linked-sialic acid and its expression is decreased with osteoclast differentiation (data not shown). Sialylation of integrin also affects the binding capacity of integrin. In the differentiation of myeloid cells along the monocyte/macrophage lineage, β_1 integrin is hyposialylated with the downregulation of ST6Gal-I expression, leading to enhanced adhesion to fibronectin [28]. Consequently, sialylation of integrins or other adhesive molecules that are expressed in osteoclast precursors, might modulate the function of these adhesive molecules. A negatively charged compound of sialic acid or an acidic condition generated by the sialylation of cell surface glycoconjugates might also affect cell–cell fusion because pH changes modulate osteoclast differentiation and activity [19].

Another possible mechanism of inhibition of osteoclast differentiation by SAase treatment is the interference of rhM-CSF or RANKL signaling because sugar chains of membranous receptor proteins sometimes affect the function of signal transmission [3,14,20]. Membrane lipid rafts, which are mainly composed of gangliosides that contain sialic acid, have a crucial role in receptor activation of nuclear factor-κB and Akt signaling in osteoclast differentiation [7,12]. Also, sialylation of cell surface glycoconjugates influences the function of the tissue necrosis factor receptor [14,31]. RANK expressed on

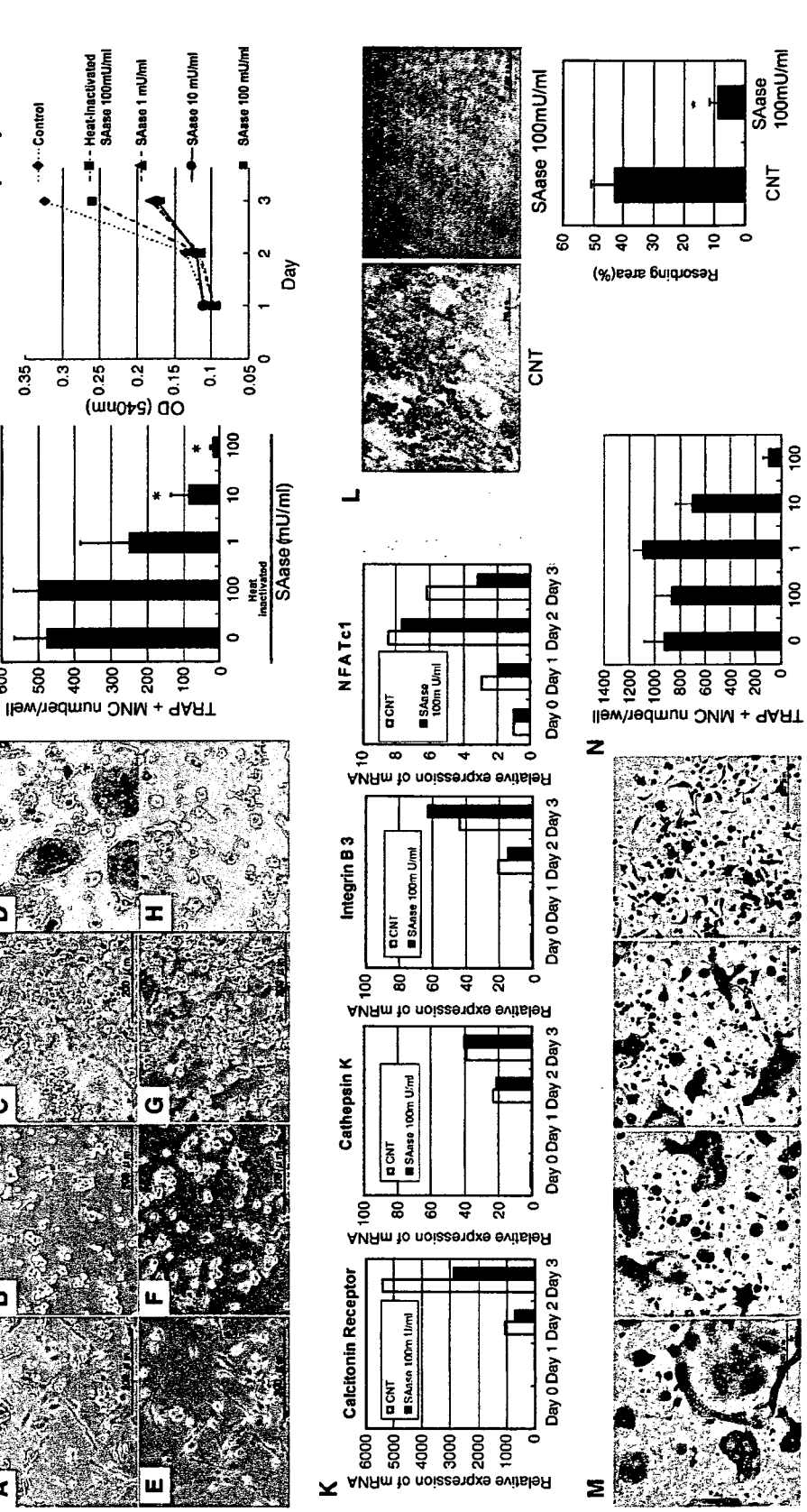

Fig. 4. (A–H) Differentiation of BMMs into mature osteoclasts. (A–D) Micrograph of mock-treated BMM cells. (E–H) Micrograph of 100 mU/ml SAase-treated BMM cells. Cells were cultured in the presence of rhM-CSF (30 ng/ml) and sRANKL (100 ng/ml) for 1 day (A and E), 2 days (B and F), and 3 days (C, D, G, and H). TRAP staining of mock or SAase-treated BMM cells after 3-day culture are shown (D or H). Original magnification, ×100. (I) Differentiation efficiency of BMM cells into TRAP-positive MNCs is shown. After 3-day culture, the number of TRAP-positive MNCs in each well of the 48-well plates was counted. (J) TRAP activity of BMM cell culture supernatant during osteoclastogenesis is shown. (K) Effect of desialylation of osteoclast precursor cells on mRNA expression of osteoclast markers during osteoclastogenesis. Calcitonin receptor, cathepsin K, integrin β3, and NFATc1 in osteoclast differentiation of BMM cells stimulated with rhM-CSF (30 ng/ml) and sRANKL (100 ng/ml). Mean values of three examinations are shown. (L) Formation of resorption pits by differentiated BMMs with or without 100 mU/ml SAase treatment in the presence of rhM-CSF (30 ng/ml) and sRANKL (100 ng/ml) for 10 days on dentin slices in 48-well plates. Original magnification, ×100. Efficacy of resorption activity of differentiated BMM cells. Slices were stained with hematoxylin and the area of the resorption pit on a dentin slice was calculated. (M) Inhibitory effect of desialylation of cell surface glycoconjugates on osteoclast differentiation in RAW 264.7 cells. Photograph of TRAP staining RAW 264.7 cells stimulated with sRANKL (50 ng/ml) after 5 days in 48-well plates, treated with SAase (0 mU/ml, 1 mU/ml, 10 mU/ml, or 100 mU/ml). Original magnification, ×100. (N) Differentiation efficacy of RAW 264.7 cells into TRAP-positive MNCs. Data are expressed as the mean and SD of the three cultures. (*, statistically different from mock-treated cells, $P<0.05$).

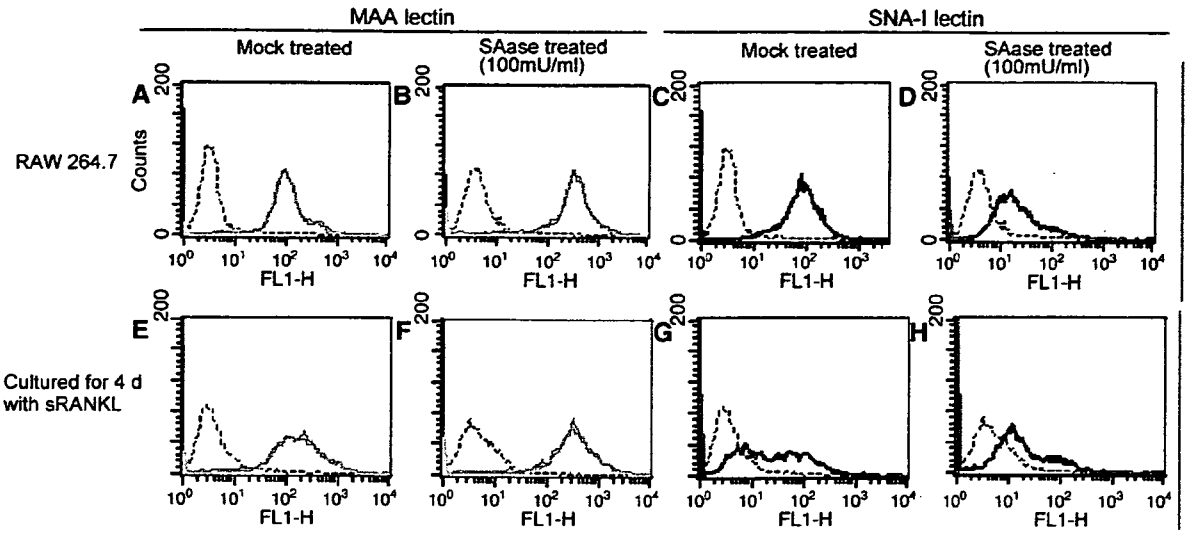

Fig. 5. Flow cytometric analyses of surface MAA lectin staining for alpha (2,3)-linked-sialic acid (A, B, E, F) and SNA-I lectin staining for alpha (2,6)-linked-sialic acid (C, D, G, H) during osteoclastogenesis with or without SAase treatment. (A–D) Upper panels show RAW264.7 cells as osteoclast precursors. (E–H) Lower panels show RAW 264.7 cells stimulated with sRANKL (50 ng/ml) after 4 days. (A, E, C, G) Mock-treated cells. (B, F, D, H) 100 mU/ml SAase-treated cells.

osteoclast precursor cells is a member of the tissue necrosis factor receptor family that encodes a 625-amino acid residue type I transmembrane protein with two potential N-linked glycosylation sites. Therefore, sialylation of RANK glycoconjugates might affect the RANKL/RANK signaling function [1]. RANKL-induced mRNA expression of osteoclast marker genes, however, was normal and TRAP-positive mononuclear cellswere formed from SAase-treated cells. Consequently, we concluded that the removal of sialic acid from cell surface glycoconjugates does not affect M-CSF or RANKL signaling in osteoclast differentiation.

It is worth mentioning that another sugar chain is involved in osteoclast cell–cell fusion. High-mannose type oligosaccharide and mannose receptors are both expressed on the cell surface of osteoclast precursors and mediate osteoclast cell–cell fusion [16,22]. The sialic acid mediated cell–cell fusion mechanism uncovered in this study is not involved in this high-mannose type oligosaccharide mediated cell–cell fusion mechanism. High-mannose type oligosaccharide does not contain sialic acid. Furthermore, Morishima et al. also reported that mannosidase I inhibitor, which inhibits the formation of complex type and hybrid type N-linked oligosaccharides that contain sialic acid, increases the formation of TRAP-positive MNCs in an osteoclastogenesis assay.

The results of this study suggested that quantitative and linkage-specific differences in sialylation of cell surface glycoconjugates regulate osteoclastic differentiation; however, there is currently little available information regarding the mechanism underlying regulation of the sialic acid content in osteoclasts or osteoclast precursors. Sialyltransferases, which reside in the Golgi apparatus, add cytidine monophosphate-activated sialic acid residues to specific terminal nonreducing positions on oligosaccharide chains of protein and lipids, but mRNA expression of ST6Gal-I showed no significant change despite the decrease of alpha (2,6)-linked-sialic acid during osteoclastgenesis. This means that there is a mechanism that degrades alpha (2,6)-linked-sialic acid during osteoclast differentiation. One possible mechanism is that endogenous SAases, which comprise four distinct forms with a predominant cellular localization (lysosomal, cytosolic, or plasma

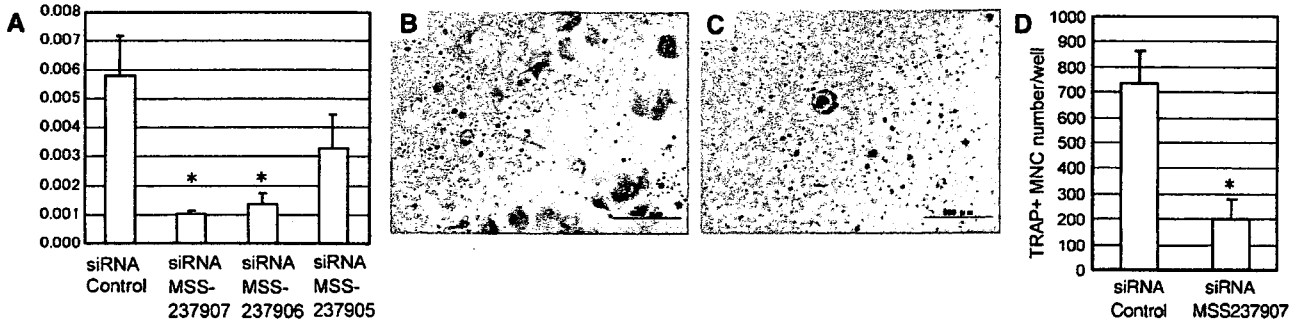

Fig. 6. Knock-down of ST6Gal-I in osteoclast precursors using siRNA and its effect on osteoclast differentiation. (A) mRNA expression level of ST6Gal-I in RAW264.7 cells at 72 h after siRNA transfection. (B) TRAP staining of RAW cells transfected with siRNA control and stimulated with sRANKL for 4 days. (C) TRAP staining of RAW cells transfected with siRNA MSS-237907 and stimulated with sRANKL for 4 days. (D) Differentiation efficiency of RAW cells into TRAP-positive MNCs is shown. Data are expressed as the mean and SD of the three experiments. (*, statistically different from siRNA control-treated cells, $P<0.05$).

membrane-associated), cleave sialic acid from glycoconjugates [21]. In monocyte/macrophage lineage cells, Stomatos et al. demonstrated the differential expression of endogenous SAases of human monocytes during cellular differentiation into macrophages [30]. However, in the differentiation process of osteoclast, there was no significant change in mRNA expression of mouse SAases (data not shown). Therefore, we speculate that alpha (2,6)-linked-sialic acid decreases as a result of the degradation or change in localization of cell surface glycoproteins or glycolipids that contains alpha (2,6)-linked-sialic acid during osteoclastgenesis. To elucidate the molecular mechanisms of alpha (2,6)-linked-sialic acid for osteoclast differentiation, further study of the regulation mechanism of the sialic acid content including identification of cell surface glycoproteins or glycolipids that contains alpha (2,6)-linked-sialic acid is necessary.

Overall, our findings demonstrate for the first time an essential role for sialic acid of cell surface glycoconjugates in the osteoclast differentiation process. Although the mechanism by which sialic acid mediates osteoclast differentiation remains unclear, alpha (2,6) linked-sialic acid is considered to be important for osteoclast cell–cell fusion. The results of this study will contribute to the future development of treatment options for bone diseases such as osteoporosis and rheumatoid arthritis.

Acknowledgments

Manufacturer Names: Wako Pure Chemical Industry Co., Ltd., Osaka, Japan; Becton Dickinson, Franklin Lakes, NJ; Corning Costar Inc., Corning, NY; Dojindo Laboratories, Kumamoto, Japan; Finnzymes Oy, Finland; Hokudo Co. Ltd., Japan; Meiji Seika, Tokyo, Japan; MJ Research, Hercules, CA; PeproTech EC, Ltd., London, U.K.; Nacalai Tesque, Inc., Kyoto, Japan; Pierce Biotechnology, Rockford, IL; Qiagen, Valencia, CA; Sigma Chemical Co., St. Louis, MO; EY Laboratories, San Mateo, CA; Cell Signaling, Beverly, MA.

References

[1] Anderson DM, Maraskovsky E, Billingsley WL, Dougall WC, Tometsko ME, Roux ER, et al. A homologue of the TNF receptor and its ligand enhance T-cell growth and dendritic-cell function. Nature 1997;390:175–9.

[2] Boyle WJ, Simonet WS, Lacey DL. Osteoclast differentiation and activation. Nature 2003;423:337–42.

[3] Bremer EG, Hakomori S, Bowen-Pope DF, Raines E, Ross R. Ganglioside-mediated modulation of cell growth, growth factor binding, and receptor phosphorylation. J Biol Chem 1984;259:6818–25.

[4] Crean SM, Meneski JP, Hullinger TG, Reilly MJ, DeBoever EH, Taichman RS. N-linked sialyated sugar receptors support haematopoietic cell-osteoblast adhesions. Br J Haematol 2004;124:534–46.

[5] Den H, Malinzak DA, Keating HJ, Rosenberg A. Influence of Concanavalin A, wheat germ agglutinin, and soybean agglutinin on the fusion of myoblasts in vitro. J Cell Biol 1975;67:826–34.

[6] Falzoni S, Chiozzi P, Ferrari D, Buell G, Di Virgilio F. P2X(7) receptor and polykarion formation. Mol Biol Cell 2000;11:3169–76.

[7] Ha H, Kwak HB, Lee SK, Na DS, Rudd CE, Lee ZH, et al. Membrane rafts play a crucial role in receptor activator of nuclear factor kappaB signaling and osteoclast function. J Biol Chem 2003;278:18573–80.

[8] Hartnell A, Steel J, Turley H, Jones M, Jackson DG, Crocker PR. Characterization of human sialoadhesin, a sialic acid binding receptor expressed by resident and inflammatory macrophage populations. Blood 2001;97:288–96.

[9] Hirohashi N, Vacquier VD. Egg sialoglycans increase intracellular pH and potentiate the acrosome reaction of sea urchin sperm. J Biol Chem 2002;277:8041–7.

[10] Illes T, Fischer J, Szabo G. Lectin histochemistry of pathological bones. Bull Hosp Jt Dis 1999;58:206–11.

[11] Ishii M, Iwai K, Koike M, Ohshima S, Kudo-Tanaka E, Ishii T, et al. RANKL-induced expression of tetraspanin CD9 in lipid raft membrane microdomain is essential for cell fusion during osteoclastogenesis. J Bone Miner Res 2006;21:965–76.

[12] Iwamoto T, Fukumoto S, Kanaoka K, Sakai E, Shibata M, Fukumoto E, et al. Lactosylceramide is essential for the osteoclastogenesis mediated by macrophage-colony-stimulating factor and receptor activator of nuclear factor-kappa B ligand. J Biol Chem 2001;276:46031–8.

[13] Keppler OT, Hinderlich S, Langner J, Schwartz-Albiez R, Reutter W, Pawlita M. UDP-GlcNAc 2-epimerase: a regulator of cell surface sialylation. Science 1999;284:1372–6.

[14] Keppler OT, Peter ME, Hinderlich S, Moldenhauer G, Stehling P, Schmitz I, et al. Differential sialylation of cell surface glycoconjugates in a human B lymphoma cell line regulates susceptibility for CD95 (APO-1/Fas)-mediated apoptosis and for infection by a lymphotropic virus. Glycobiology 1999;9:557–69.

[15] Kukita T, Wada N, Kukita A, Kakimoto T, Sandra F, Toh K, et al. RANKL-induced DC-STAMP is essential for osteoclastogenesis. J Exp Med 2004;200:941–6.

[16] Kurachi T, Morita I, Oki T, Ueki T, Sakaguchi K, Enomoto S, et al. Expression on outer membranes of mannose residues, which are involved in osteoclast formation via cellular fusion events. J Biol Chem 1994;269:17572–175876.

[17] Mbalaviele G, Chen H, Boyce BF, Mundy GR, Yoneda T. The role of cadherin in the generation of multinucleated osteoclasts from mononuclear precursors in murine marrow. J Clin Invest 1995;95:2757–65.

[18] McInnes A, Rennick DM. Interleukin 4 induces cultured monocytes/macrophages to form giant multinucleated cells. J Exp Med 1988;167:598–611.

[19] Meghji S, Morrison MS, Henderson B, Arnett TR. pH dependence of bone resorption: mouse calvarial osteoclasts are activated by acidosis. Am J Physiol: Endocrinol Metab 2001;280:E112–9.

[20] Meuillet EJ, Kroes R, Yamamoto H, Warner TG, Ferrari J, Mania-Farnell B, et al. Sialidase gene transfection enhances epidermal growth factor receptor activity in an epidermoid carcinoma cell line, A431. Cancer Res 1999;59:234–40.

[21] Miyagi T, Wada T, Yamaguchi K, Hata K. Sialidase and malignancy: a minireview. Glycoconj J 2004;20:189–98.

[22] Morishima S, Morita I, Tokushima T, Kawashima H, Miyasaka M, Omura K, et al. Expression and role of mannose receptor/terminal high-mannose type oligosaccharide on osteoclast precursors during osteoclast formation. J Endocrinol 2003;176:285–92.

[23] Moscona A, Peluso RW. Fusion properties of cells persistently infected with human parainfluenza virus type 3: participation of hemagglutinin-neuraminidase in membrane fusion. J Virol 1991;65:2773–7.

[24] Murch AR, Grounds MD, Marshall CA, Papadimitriou JM. Direct evidence that inflammatory multinucleate giant cells form by fusion. J Pathol 1982;137:177–80.

[25] Namba K, Nishio M, Mori K, Miyamoto N, Tsurudome M, Ito M, et al. Involvement of ADAM9 in multinucleated giant cell formation of blood monocytes. Cell Immunol 2001;213:104–13.

[26] Primakoff P, Myles DG. Penetration, adhesion, and fusion in mammalian sperm–egg interaction. Science 2002;296:2183–5.

[27] Schadee-Eestermans IL, Hoefsmit EC, van de Ende M, Crocker PR, van den Berg TK, Dijkstra CD. Ultrastructural localisation of sialoadhesin (siglec-1) on macrophages in rodent lymphoid tissues. Immunobiology 2000;202:309–25.

[28] Semel AC, Seales EC, Singhal A, Eklund EA, Colley KJ, Bellis SL. Hyposialylation of integrins stimulates the activity of myeloid fibronectin receptors. J Biol Chem 2002;277:32830–6.

[29] Stamatos NM, Curreli S, Zella D, Cross AS. Desialylation of glycoconjugates on the surface of monocytes activates the extracellular signal-related kinases ERK 1/2 and results in enhanced production of specific cytokines. J Leukoc Biol 2004;75:307–13.

[30] Stamatos NM, Liang F, Nan X, Landry K, Cross AS, Wang LX, et al. Differential expression of endogenous sialidases of human monocytes during cellular differentiation into macrophages. FEBS J 2005;272: 2545–56.

[31] Suzuki O, Nozawa Y, Abe M. Sialic acids linked to glycoconjugates of Fas regulate the caspase-9-dependent and mitochondria-mediated pathway of Fas-induced apoptosis in Jurkat T cell lymphoma. Int J Oncol 2003;23:769–74.

[32] Suzuki Y, Nagao Y, Kato H, Matsumoto M, Nerome K, Nakajima K, et al. Human influenza A virus hemagglutinin distinguishes sialyloligosaccharides in membrane-associated gangliosides as its receptor which mediates the adsorption and fusion processes of virus infection. Specificity for oligosaccharides and sialic acids and the sequence to which sialic acid is attached. J Biol Chem 1986;261:17057–61.

[33] Tajima M, Higuchi S, Higuchi Y, Miyamoto N, Uchida A, Ito M, et al. Suppression of FRP-1/CD98-mediated multinucleated giant cell and osteoclast formation by an anti-FRP-1/CD98 mAb, HBJ 127, that inhibits c-src expression. Cell Immunol 1999;193: 162–9.

[34] Takeshita S, Kaji K, Kudo A. Identification and characterization of the new osteoclast progenitor with macrophage phenotypes being able to differentiate into mature osteoclasts. J Bone Miner Res 2000;15: 1477–88.

[35] Udagawa N, Takahashi N, Jimi E, Matsuzaki K, Tsurukai T, Itoh K, et al. Osteoblasts/stromal cells stimulate osteoclast activation through expression of osteoclast differentiation factor/RANKL but not macrophage colony-stimulating factor: receptor activator of NF-kappa B ligand. Bone 1999;25:517–23.

[36] Varki A. Sialic acids as ligands in recognition phenomena. FASEB J 1997;11:248–55.

[37] Vignery A. Osteoclasts and giant cells: macrophage–macrophage fusion mechanism. Int J Exp Pathol 2000;81:291–304.

[38] Yagi M, Miyamoto T, Sawatani Y, Iwamoto K, Hosogane N, Fujita N, et al. DC-STAMP is essential for cell–cell fusion in osteoclasts and foreign body giant cells. J Exp Med 2005;202:345–51.

Mod Rheumatol (2007) 17:322–326
DOI 10.1007/s10165-007-0590-y

ORIGINAL ARTICLE

**Takafumi Yayama · Shigeru Kobayashi · Yasuo Kokubo
Tomoo Inukai · Yasutaka Mizukami · Masafumi Kubota
Jyunichi Ishikawa · Hisatoshi Baba · Akio Minami**

Motion analysis of the wrist joints in patients with rheumatoid arthritis

Received: January 12, 2007 / Accepted: May 1, 2007

Abstract We investigated the characteristics of the wrist joint motion in patients with rheumatoid arthritis (RA), using a biaxial flexible goniometer. Wrist joint range of motion and velocity were measured on the dominant hand in RA patients ($n = 22$) and normal individuals ($n = 5$). We investigated flexion–extension (FE) task, radial–ulnar deviation (RUD) task, and functional motion tasks, such as writing letters or unscrewing the lid of a jar. In normal individuals, there was cooperative coupling of FE and RUD during wrist movement, and this coupling motion was essential for normal wrist movements. On the other hand, in RA patients, wrist joint range of motion was restricted at various degrees, with reduced joint motion velocity that was severe on RUD. Functional wrist motion tasks indicated circumductive movement with both FE and RUD in normal individuals, whereas the direction of movement was limited in RA patients, and results revealed failure of cooperative coupling of FE and RUD. Our results indicate that disturbed coupling of FE and RUD results in difficulties in the cooperative movements and have great influence on the daily activities in RA wrist joint.

Key words Biomechanics · Motion analysis · Rheumatoid arthritis · Wrist joint

Introduction

The wrist joint is involved in rheumatoid arthritis (RA) especially in patients with advanced disease. In daily clinical practice, it is essential to assess the anatomical conditions and impairment of the rheumatoid wrist joint followed by appropriate medical and physical therapies to maintain the patient's daily activities. It is obviously important to treat pain and its associated joint movement limitations, including the selection of appropriate treatment option.

The available surgical treatments for rheumatic wrist joints include synovectomy, resection arthroplasty, and arthrodesis, with suitability of each dependent upon the patient.[1,2] These surgical procedures may be performed on the basis of destructive conditions of the wrist joints, with a particular goal of increasing joint motion and elimination of motion pain. Various resection arthroplasty procedures and their modifications have been described, but each carries both advantages and disadvantages. Total joint arthroplasty is useful for the replacement of joints in destructive disease involving the hip or knee joints, both in terms of pain control and preservation of range of motion. However, in the wrist joint, prostheses lacks longevity and histocompatibility.[3–5] Total wrist arthroplasty has also been found to be unsuitable for severe joint malformation, chronic subluxion, and collapse of the carpal bone.[6] It is clear that optimum treatments are required for each stage of RA joint destruction.

The purpose of this study was to describe the two-dimensional in vivo behavior of rheumatic wrist joints using a biaxial goniometer. This analysis and assessment of the dynamic function of the wrist joint may be useful for allowing the RA patient appropriate joint motion in daily activities.

T. Yayama (✉) · S. Kobayashi · Y. Kokubo · T. Inukai · Y. Mizukami · M. Kubota · H. Baba
Department of Orthopaedics and Rehabilitation Medicine, Fukui University Faculty of Medical Sciences, 23 Matsuoka Shimoaizuki, Eiheiji, Fukui 910-1193, Japan
Tel. +81-776-61-8383; Fax +81-776-61-8125
e-mail: yayama@u-fukui.ac.jp

J. Ishikawa · A. Minami
Department of Orthopaedic Surgery, Division of Advanced Medical Sciences, Hokkaido University Graduate School of Medicine, Sapporo, Japan

Materials and methods

Subjects

We conducted a motion analysis of the wrist joint in 22 RA patients who complained of pain and swelling. Patients were 2 men and 20 women, with an average age of 60.1 years (range, 29–74 years) at the time of the current analysis. All subjects satisfied the American College of Rheuma-

tology 1987 revised criteria for RA,[7] and had no history of trauma, surgical treatment for the wrist joint, or neuropathy in the upper extremity. With regard to Larsen's radiographic classification, five patients had grade II conditions, six grade III, nine grade IV, and two grade V. Control subjects were five women of an average age of 25.2 years (range, 22–27 years) who had no destructive joint changes. The study protocol strictly followed the Ethics Review Committee Guidelines of our University Hospital, and written informed consent was obtained from all patients and control volunteers.

Experimental procedures

Wrist joint range of motion and velocity were measured on the patient's dominant hand (all subjects were right handed) using a biaxial goniometer (M100; Penny & Giles Blackwood, Gwent, UK). Markers were attached to the skin with adhesive tapes. The distal goniometry marker was placed along the third metacarpal bone, and the proximal maker was placed on the dorsal surface of the forearm along the radius.[8] After the attachment of the markers, the subject was seated with their humerus positioned at 0° abduction in the frontal plane and 0° flexion in the sagittal plane. The elbow joint was held at 90° of flexion and the forearms positioned at 0° of pronation (Fig. 1). During the flexion–extension (FE) task, the patient performed maximal flexion and extension at one cycle per second, paced by a metronome. The radial–ulnar deviation (RUD) task was similar to the FE task, except that the motion was in the radial–ulnar direction. Patients performed functional motion tasks, such as writing letters and unscrewing the lid of a jar, at their own speed.

Data processing and analysis

A neutral wrist position is defined as the 0° FE and 0° RUD when the axis of forearm and middle finger are in parallel. The FE and RUD tasks were performed at a sampling frequency of 200 Hz, and the motion angle and motion angle speed for the 6th to the 15th cycle of a total of 20 cycles were used for analysis. Subsequent analyses were conducted with a 2-channel analogue amplifier (AD Instruments Japan, Tokyo, Japan) and a Power Lab system (AD Instruments Japan). Mann–Whitney U-test and analysis of variance were used to analyze the results. The level of significance was $P < 0.05$.

Results

Flexion–extension task

Figure 2a shows a representative case of a 38-year-old woman who presented Larsen's radiographic classification

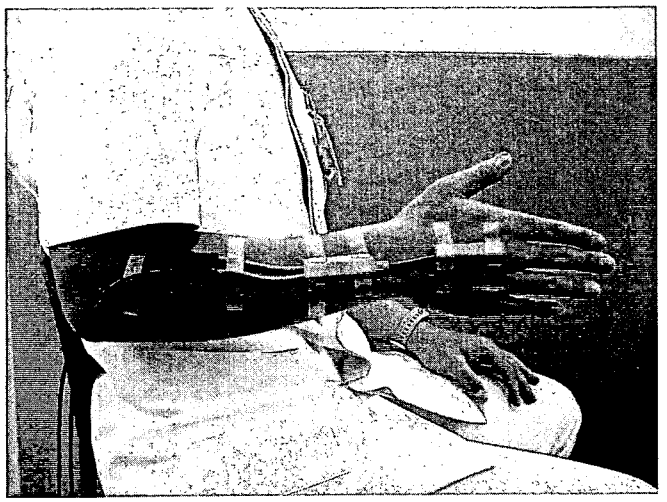

Fig. 1. Goniometry markers were placed on the forearm and hand. The subject was seated with the humerus positioned at 0° abduction and 0° flexion. The elbow joint was held at 90° of flexion and the forearms positioned at 0° of pronation

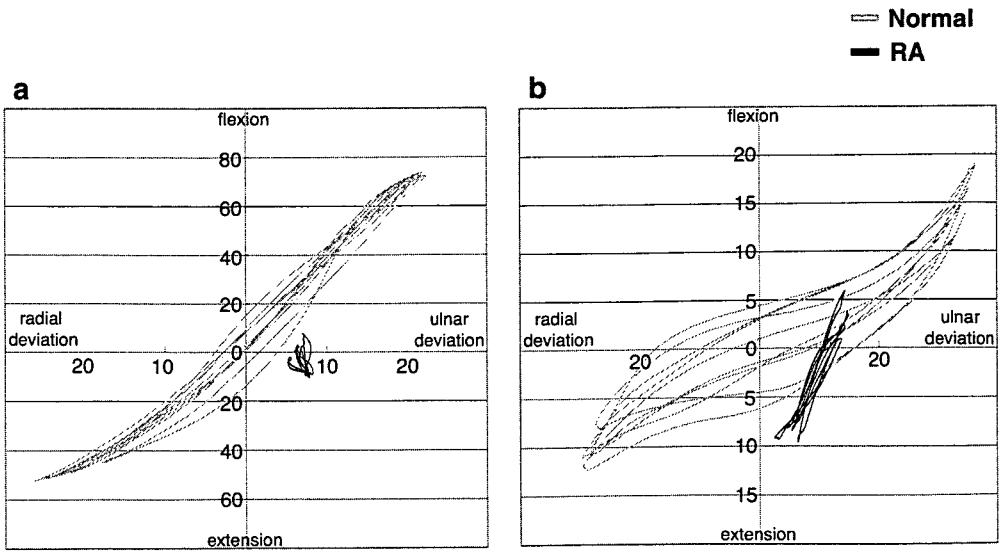

Fig. 2. Representative motion for angle–angle plots and their regression lines during flexion–extension (FE) (**a**) and radial–ulnar deviation (RUD) (**b**) trials. Rheumatoid arthritis (*RA*) patients (38 year-old woman, Larsen grade III) showed limited range of motion, and cooperative FE and RUD motion compared with normal individuals (22-year-old woman)

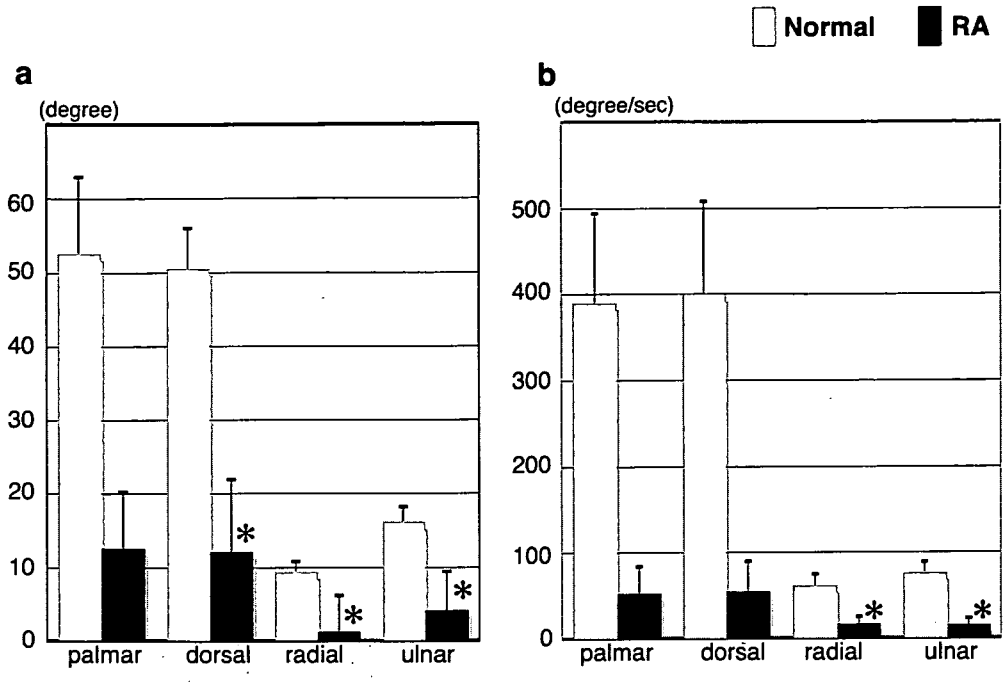

Fig. 3. Range of motion (**a**) and velocity (**b**) during FE tasks. There were significant differences in the range of motion on extension, radial-ulnar deviation and velocity on radial–ulnar deviation (* $P < 0.05$)

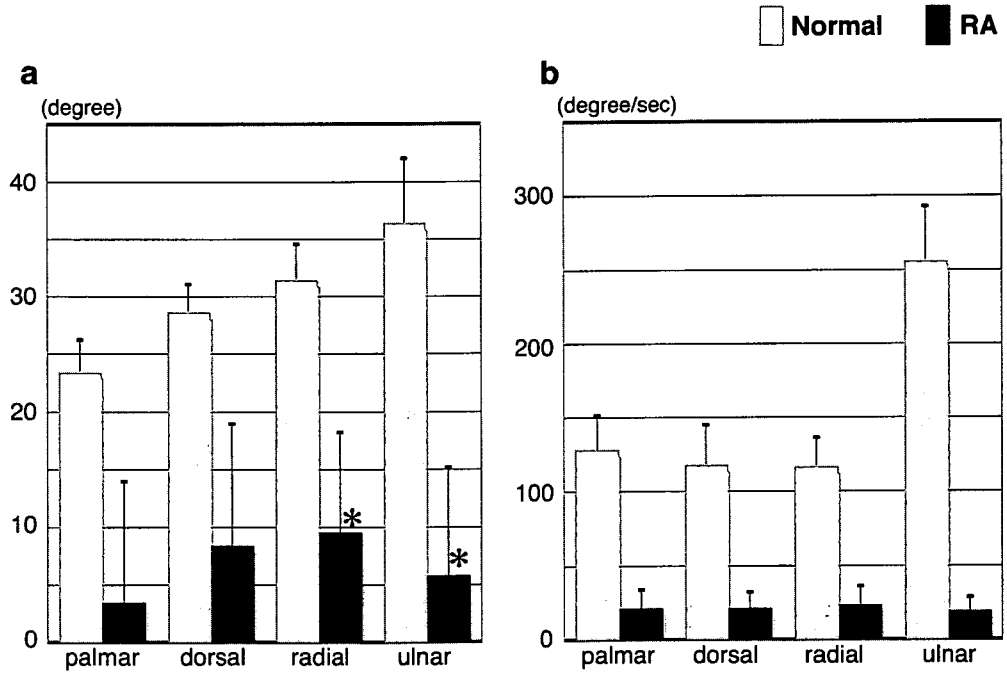

Fig. 4. Range of motion (**a**) and velocity (**b**) during RUD tasks. There was a significant difference in the range of motion on radial–ulnar deviation (* $P < 0.05$)

grade III. During the FE task, RA patients showed limited range of motion and cooperative FE and RUD motion of the wrist joint compared with normal individuals. Patients with RA exhibited a restricted wrist movement, especially for extension, radial deviation, and ulnar deviation (Fig. 3a). In addition, reduced performance in the FE task increased with the progression of joint destruction. Analysis of joint velocity showed marked impairment of directed radial-ulnar movement. The velocity of radial deviation was 15.8°/s in RA patients and 76.4°/s in normal individuals, while ulnar deviation was 16.7°/s in RA patients and 61.1°/s in normal individuals (Fig. 3b).

Radial–ulnar deviation task

During the RUD task, the control subject demonstrated a coupling of FE and RUD, which was reduced in the RA patient, similar to the findings in the FE task (Fig. 2b). Figure 4 shows the results of analysis of variance for RUD (Fig. 4a, range of motion; Fig. 4b, velocity). The average range of motion for radial deviation was 9.5° in RA patients and 31.5° in normal individuals, and radial deviation was 5.8° in RA patients and 36.4° in normal individuals. The velocity of RUD was reduced in all directions, though there were no significant differences between RA patients and

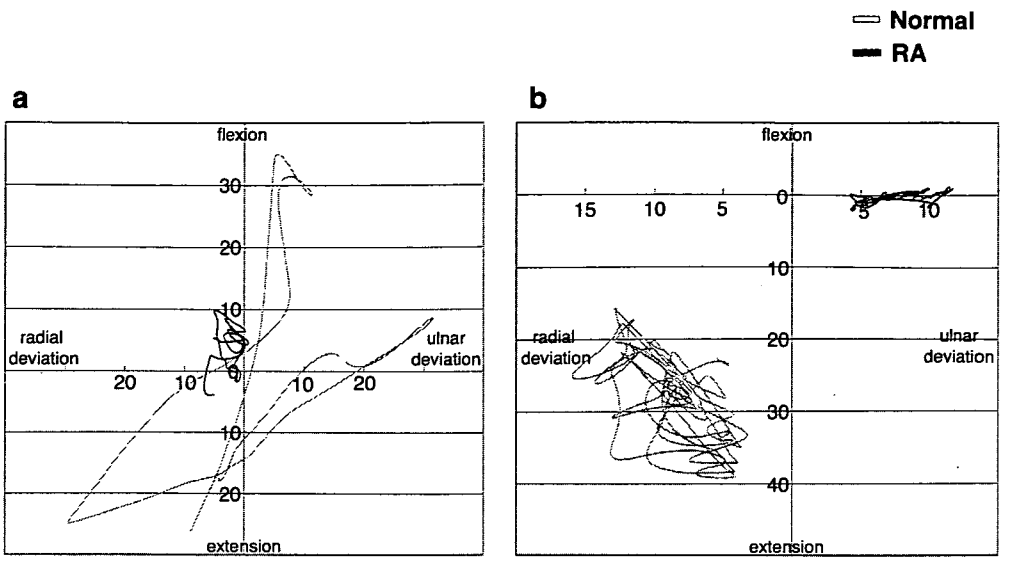

Fig. 5. Example of functional motion (**a**: unscrewing the lid of a jar; **b**: writing) in normal (22-year-old woman) and rheumatoid arthritis (*RA*) wrist joint (42-year-old woman, Larsen grade IV). Rheumatoid arthritis patient showed disturbance of the circumductory motion

control individuals. The range of motion and velocity tended to be reduced in proportion to the degree of joint destruction, and the relationship between Larsen's radiographic classification and RUD task parameters was insignificant.

Functional motion (unscrewing lid of a jar or writing letters)

In normal individuals, the wrist joint presented the boundary of motion in all directions, that the third metacarpal bone roundly moved to the axis of radius with circumduction cycles, when they unscrewed the lid of a jar. Figure 5a shows representative data of unscrewing from a 42-year-old woman with Larsen grade IV. The range of motion and velocity of wrist movement were severely limited in the study patients, and the wrist circumduction cycle was small. The RA patient tended to undergo a decrease of circumduction cycles to the extent of joint destruction. During writing, the normal wrist showed circumduction, with extension being the dominant direction of movement. Rheumatoid arthritis patients kept their wrist joint in a neutral or slightly flexed position, and writing was carried out by radial–ulnar deviation with an ulnar drift. The magnitude of the circumduction cycle was small or zero, as shown in the representative result illustrated in Fig. 5b.

Discussion

The wrist joint is a biaxial joint with two degrees of direction: a flexion–extension motion and a radial–ulnar deviation. The present study showed that cooperative coupling of FE and RUD was important for normal wrist movement.[9,10] Although a small amount of axial rotation may exist in FE and RUD, this motion has little effect and does not generally occur at the level of the wrist complex.[11,12] In our study, the primary FE motion necessitated comparable secondary motion in RUD, and the primary RUD also necessitated secondary motion in FE, as indicated by the slope of the regression line during FE or RUD tasks in the control wrist. These movements corresponding to extension with radial deviation and flexion with ulnar deviation (similar to the motion of a dart thrower) support a plane oblique to the anatomical planes and facilitate wrist mobility and agility. This coupling of FE and RUD has a large impact on the ability of patients to perform many activities of daily living, involved in many functional tasks such as hair combing, washcloth wringing, shoelace tying, and can-opening.[12]

The main factors that limit and affect wrist motion patterns include irregularity of articular carpal bone surfaces, constraints of carpal ligaments, and muscle contraction patterns.[13–15] Rheumatoid arthritis patients in the present study had a severely reduced range of motion and velocity of movement in the direction of radial–ulnar deviation during the FE task, and a restricted range of motion in radial deviation and ulnar deviation during the RUD task. These results indicate that the restriction of movement in the direction of radial–ulnar deviation caused by RA joint destruction may lead to imbalance of cooperative coupling of FE with RUD, and these imbalances are associated with difficulties in achieving smooth movement of the wrist joint.

The circumductive wrist motion, which was induced by cooperative FE and RUD coupling, also plays an important role in the capacity for daily activities. We presume that the velocity presented in this study may reflect the natural wrist motion of circumduction. Evans et al.[16] reported that the motion of the hand segment relative to the forearm segment during FE and RUD was of smaller magnitude in RA patients than in normal individuals. In our study, RA patients showed severely limited velocity in all directions of wrist motion and exhibited little wrist circumduction on writing or unscrewing of a jar. In addition, ulnar drift defor-

mity may also influence these motion impairments, because the wrist has the greatest range at the anatomically neutral position on circumduction.[17] These results indicate that appropriate stability of the radial-ulnar deviation is particularly important in the functional outcome of RA wrist joint movement. However, surgical stabilization of the radial–ulnar deviation may limit the range of wrist movement. Palmer et al.[12] showed that the range of wrist joint movement required for activities of daily living was 30° of dorsal flexion and 5° of palmar flexion. We consider that stabilization of radial-ulnar deviation is more important in reconstruction of the RA wrist joint than maximization of the flexion-extension range.

There are a number of limitations to this study. The wrist joint range of motion and velocity tended to be limited, and the wrist circumduction cycle was reduced in proportion to the degree of joint destruction in patients with RA. Because our study group was small, and pain and/or soft tissue imbalance may have affected wrist joint mobility, we could not assess the relationship between wrist joint function/kinematics and the stage of progression of destructive RA. Knowledge of the relationship between the grade of joint destruction and wrist kinematics is necessary for the determination of appropriate treatment. Further evaluation of the functional and dynamic motion of the wrist joint is needed.

In conclusion, the coupling motion of FE and RUD is important for natural wrist movement. There is a preferable wrist motion pattern that combines extension with radial deviation and flexion with ulnar deviation during daily tasks. Wrist joint destruction in RA severely affects the range of motion and velocity for RUD. We postulate that these imbalances of FE and RUD coupling motion greatly influence daily activities in RA wrist joint.

Acknowledgments This work was supported in part by a grant from the Investigation Committee on Rheumatoid arthritis, the Public Health Bureau of the Ministry of Health and Welfare of the Japanese Government.

References

1. Ishikawa H, Murasawa A, Nakazono K. Long-term follow-up study of radiocarpal arthrodesis for the rheumatoid wrist. J Hand Surg (Am) 2005;30:658–66.
2. Nakamura H, Tanaka H, Yoshino S. Long-term results of multiple synovectomy for patients with refractory rheumatoid arthritis. Effects on disease activity and radiological progression. Clin Exp Rheumatol 2004;22:151–7.
3. Cobb TK, Beckenbaugh RD. Biaxial total-wrist arthroplasty. J Hand Surg (Am) 1996;21:1011–21.
4. Meuli HC, Fernandez DL. Uncemented total wrist arthroplasty. J Hand Surg (Am) 1995;20:115–22.
5. Swanson AB. Flexible implant arthroplasty for arthritic disabilities of the radiocarpal joint. Orthop Clin North Am 1973;4:383–94.
6. Takwale VJ, Nuttall D, Trail IA, Stanley JK. Biaxial total wrist replacement in patients with rheumatoid arthritis. J Bone Joint Surg (Br) 2002;84:692–9.
7. Arnett FC, Edworthy SM, Bloch DA, McShane DJ, Fries JF, Cooper NS, et al. The American Rheumatism Association 1987 revised criteria for the classification of rheumatoid arthritis. Arthritis Rheum 1988;31:315–24.
8. Ojima H, Miyake S, Kumashiro M, Togami H, Suzuki K. Dynamic analysis of wrist circumduction: a new application of the biaxial flexible electrogoniometer. Clin Biomech 1991;6:221–9.
9. Andrews JG, Youm Y. A Biomechanical investigation of wrist kinematics. J Biomech 1979;12:83–93.
10. Youm Y, McMurthy RY, Flatt AE, Gillespie TE. Kinematics of the wrist. An experimental study of radial-ulnar deviation and flexion-extension. J Bone Joint Surg (Am) 1978;60:423–31.
11. Li ZM. The influence of wrist position on individual finger forces during forceful grip. J Hand Surg (Am) 2002;27:886–96.
12. Palmer AK, Werner FW, Murphy D, Glisson R. Functional wrist motion: a biomechanical study. J Hand Surg (Am) 1985;10:39–46.
13. Ishikawa J, Cooney WP, Niebur G, An KN, Minami A, Kaneda K. The effects of wrist distraction on carpal kinematics. J Hand Surg (Am) 1999;24:113–20.
14. Sennwald GR, Zdravkovic V, Jacob HA, Kern HP. Kinematics analysis of relative motion within the proximal carpal row. J Hand Surg (Br) 1993;18:609–12.
15. Volz RG, Lieb M, Benjamin J. Biomechanics of the wrist. Clin Orthop Relat Res 1980;149:112–7.
16. Evans JS, Blair WF, Andrews JG, Crowninshield RD. The in vivo kinematics of the rheumatoid wrist. J Orthop Res 1986;4:142–51.
17. Li ZM, Kuxhaus L, Fisk JA, Christophel TH. Coupling between wrist flexion-extension and radial-ulnar deviation. Clin Biomech 2005;20:177–83.

Donor Site Evaluation After Autologous Osteochondral Mosaicplasty for Cartilaginous Lesions of the Elbow Joint

Norimasa Iwasaki,*† MD, PhD, Hiroyuki Kato,‡ MD, PhD, Tamotsu Kamishima,§ MD, PhD, Naoki Suenaga,† MD, PhD, and Akio Minami,† MD, PhD
From the †Department of Orthopaedic Surgery, Hokkaido University School of Medicine, Sapporo, Japan, ‡Department of Orthopaedic Surgery, Shinsyu University School of Medicine, Matsumoto, Japan, and §Department of Radiology, Hokkaido University School of Medicine, Sapporo, Japan

Background: One significant disadvantage of autologous osteochondral mosaicplasty (mosaicplasty) is the harvesting of osteochondral grafts from the normal articular area of the knee joint. However, the effect of harvesting grafts on knee function remains unclear.

Purpose: To clarify the functional effects on the donor knee of harvesting osteochondral grafts and to perform magnetic resonance imaging evaluation of donor site repair after mosaicplasty for capitellar osteochondritis dissecans in young athletes.

Study Design: Case series; Level of evidence, 4.

Methods: Eleven male competitive athletes with advanced lesions of capitellar osteochondritis dissecans underwent mosaicplasties. The surgical technique involves obtaining small-sized cylindrical osteochondral grafts from the lateral periphery of the femoral condyle at the level of the patellofemoral joint and transplanting them to osteochondral defects in the capitellum. Assessment at a mean follow-up of 26 months included local findings of the donor knees, a Lysholm knee scoring scale, International Knee Documentation Committee standard evaluation form, and magnetic resonance imaging evaluation.

Results: All patients returned to a competitive level of their previous sports without any donor site disturbances. Based on the Lysholm knee score and International Knee Documentation Committee evaluation form, all knees were graded as excellent and normal, respectively. The magnetic resonance imaging showed 50% to 100% defect fill in 6 of 9 patients and normal or nearly normal signals in 4 patients at the donor sites.

Conclusion: No adverse effects of osteochondral graft harvest on donor knee function were found after mosaicplasty for capitellar osteochondritis dissecans in young athletes. However, magnetic resonance imaging indicates that the donor site is resurfaced with fibrous tissue.

Keywords: mosaicplasty; donor site; osteochondritis dissecans (OCD); elbow joint; knee joint

Because of the limited capacity for self-repair of articular cartilage, treatment of articular defects has been challenging. Autologous osteochondral mosaicplasty (mosaicplasty) is an innovative technique to transplant multiple cylindrical osteochondral grafts harvested from a less weightbearing area of the knee joint into the chondral defects.[6-8,15] Previous studies[6,7,11,12,14] reported the successful treatment of osteochondral defects in knee and ankle joints with this surgical technique.

Recent studies[10,19,23] have reported the application of mosaicplasty to osteochondritis dissecans of the humeral capitellum (capitellar OCD). Iwasaki et al[10] have shown that mosaicplasty for advanced capitellar OCD with displaced and detached fragments in teenage baseball players can provide excellent clinical and radiographic results. Although mosaicplasty is effective for capitellar OCD as well as osteochondral defects in the knee joint, surgeons must consider the possible adverse effect on the donor sites in performing this procedure, especially for young athletes.

To date, only a few studies[6,7,13,17] have reported on the morbidity at the graft harvest sites in doing mosaicplasty for knee cartilaginous lesions. Therefore, the effect on knee

*Address correspondence to Norimasa Iwasaki, MD, PhD, Department of Orthopaedic Surgery, Hokkaido University School of Medicine, Kita 15, Nishi 7, Sapporo 060-8638, Japan (e-mail: niwasaki@med.hokudai.ac.jp).

No potential conflict of interest declared.

The American Journal of Sports Medicine, Vol. 35, No. 12
DOI: 10.1177/0363546507306465

function after osteochondral graft harvest is still controversial. The objectives of this study were to clarify the functional effects of osteochondral graft harvest on the donor knee and to perform MRI evaluation of donor site repair after mosaicplasty for advanced lesions of capitellar OCD in young athletes. When compared with previous studies, the results obtained here will provide surgeons more accurate information on the morbidity that ensues at the graft donor harvest sites because the donor and diseased joint are completely separated.

MATERIALS AND METHODS

Subjects

A retrospective chart review at the senior author's institution identified 13 male patients (13 elbows) with advanced lesions of capitellar OCD who underwent mosaicplasty between March 1993 and October 2005. All patients, except for 2 who had not been followed up for a minimum of 12 months, were included in this study. All 11 remaining patients were competitive athletes (baseball, 8 patients; rugby, 1; American football, 1; soccer, 1) at the time of operation. Their mean age at the time of surgery was 14 years (range, 11-22 years). No patients had any history of severe trauma or symptoms in the donor knee.

Operative Technique

All operations were performed under general anesthesia by the senior authors according to the surgical technique described previously.[10] After the capitellar OCD lesion was exposed, the fragment was raised using a chisel, and the subchondral fibrous tissue was curetted. By tapping a drill guide down to viable subchondral bone, optimal filling of the defect could be projected. The mean surface area of the defect was 145.4 mm^2 (range, 49-270 mm^2). To harvest cylindrical grafts, the surgeon performed a lateral parapatellar mini-arthrotomy of the contralateral knee to the operated elbow. With a properly sized tubular chisel, small (2.7-6.0 mm in diameter, 10-15 mm in length) cylindrical grafts were obtained from the lateral periphery of the femoral condyle at the level of the patellofemoral joint (Figure 1). The mean total surface area of grafts was 33.7 mm^2 (range, 15.3-56.5 mm^2). The harvested grafts were transplanted to prepared osteochondral defects in the capitellum. In 3 patients, 5 grafts were harvested for reconstruction; in 2 patients, 4 grafts; in 2 patients, 3 grafts; and in 4 patients, 2 grafts. Each donor site was packed with bone wax to prevent postoperative bleeding, and a drain was inserted. Postoperatively, the drain was removed at 24 or 48 hours. The patients were instructed in a less weightbearing gait at 2 days and allowed to walk freely at 7 days postoperatively. We did not direct the patients to do any specific rehabilitation for the knee.

Postoperative Evaluation

All patients were subjected to a standardized history and physical examination by the senior author at follow-up.

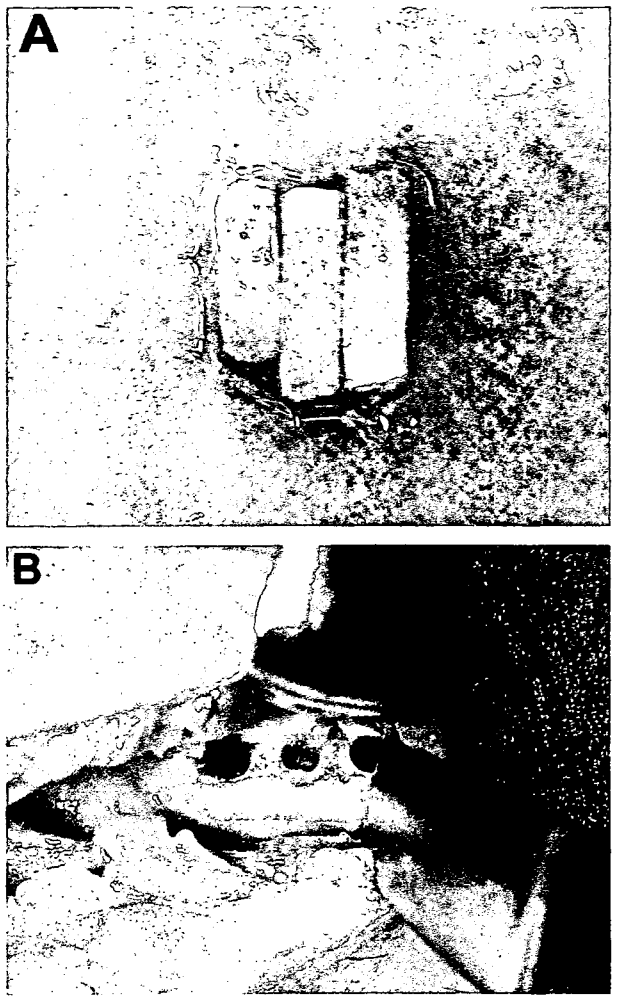

Figure 1. Small cylindrical osteochondral plugs (A) are harvested from the lateral less weightbearing periphery of the femoral condyle at the level of the patellofemoral joint (B).

Follow-up assessment included local findings of the donor knee, a Lysholm knee scoring scale,[21] an International Knee Documentation Committee (IKDC) standard evaluation form (objective),[3] completion of a questionnaire regarding the athlete's return to sports, and MRI evaluation. The range of extension and flexion of the knee as well as the thigh and calf girth were measured and expressed as a percentage of the contralateral side. The points according to the Lysholm score (0-100 points) were graded as excellent (>94 points), good (84-94 points), fair (60-83 points), or poor (<60 points). Based on the IKDC standard evaluation form, knees were graded as normal (A), nearly normal (B), abnormal (C), or severely abnormal (D). The quality of the donor site repair was semiquantitatively assessed from MRI findings according to the scoring system of Henderson et al[9] (Table 1). The MRI sequences according to the report by Roberts et al[18] were undertaken using a Siemens Vision 1.5-T scanner (Siemens, Erlangen, Germany) with a gradient strength of 25 mT/m and VB33A software. The score was based on a review by a musculoskeletal radiologist. The radiologist was masked to clinical results.

TABLE 1
The Magnetic Resonance Imaging Scoring System of Henderson et al[9]

Feature	MRI Score, point 1	2	3	4
Fill of the repair site	Complete	>50% of the defect	<50% of the defect	Full-thickness defect
Signal at the repair site	Normal (identical to adjacent articular cartilage)	Nearly normal (slight areas of hyperintensity)	Abnormal (large areas of hyperintensity)	Absent
Bone marrow edema	Absent	Mild	Moderate	Severe
Effusion	Absent	Mild	Moderate	Severe

TABLE 2
Patient Descriptions and Postoperative Clinical Results of Donor Knee After Graft Harvest

Patient Number	Age, y	Sport	Size, mm × No. of Graft (diameter × no.)	Follow-up, mo	Lysholm Knee Score, points	International Knee Documentation Committee Evaluation Form
1	14	Baseball	4.5 × 2; 2.7 × 1	65	100	Normal
2	16	Rugby	3.5 × 1; 2.7 × 1	55	100	Normal
3	15	Baseball	6 × 2	25	100	Normal
4	11	Baseball	3.5 × 3	28	100	Normal
5	13	Baseball	3.5 × 2	26	100	Normal
6	14	Baseball	3.5 × 1; 2.7 × 4	22	100	Normal
7	22	American football	3.5 × 3; 2.7 × 1	17	100	Normal
8	12	Soccer	3.5 × 3; 2.7 × 1	14	100	Normal
9	15	Baseball	3.5 × 2	13	96	Normal
10	14	Baseball	3.5 × 4; 2.7 × 1	12	100	Normal
11	12	Baseball	3.5 × 5	12	100	Normal

Statistical Analysis

Statistical comparisons were performed using paired *t* tests. The level of significance was set at a probability value less than .05.

RESULTS

Postoperative results, along with patient data, are summarized in Table 2. Mean total amount of bleeding from the operated knee joint was 17.4 mL (range, 8-43 mL). In 8 patients (73%), the joint effusion persisted for a mean of 3 weeks (range, 1-5 weeks) after operation. At a mean follow-up of 26 months (range, 12-65 months), no patients except 1 had any symptoms or local findings of the knee. The remaining 1 patient had slight knee pain with stair climbing. In all patients, the percentage of range of extension and flexion of the knee was 100%. The thigh girth, at 5 and 10 cm proximal to the superior edge of the patella, and calf girth compared with the opposite limb were 99.7% (range, 96.8%-102.7%), 99.7% (range, 97.2%-101.2%), and 100.3% (range, 96.9%-101.5%), respectively. All patients returned to the competitive level of their previous sports without any donor site disturbances. The Lysholm knee score was 99.6 points (range, 96-100 points), and all patients were graded as excellent. According to the IKDC evaluation form, all knees were characterized as normal (A). Based on the rating system of Timmerman and Andrews,[22] the mean clinical score of the operated elbow significantly improved from 132.3 points (range, 75-155 points) to 185.9 points (range, 145-200 points) postoperatively ($P < .001$). Overall evaluation results were excellent in 9 patients, good in 1 patient, and fair in 1 patient.

TABLE 3
Postoperative Magnetic Resonance Imaging Scores of Each Patient[a]

Patient No.	Point: Fill of the Repair Site	Signal at the Repair Site	Bone Marrow Edema	Effusion	Overall Score
1	1	2	1	1	5
2	2	2	1	1	6
3	2	3	1	1	7
4	2	3	1	1	7
6	2	2	1	1	6
8	1	1	1	1	4
9	3	3	1	1	8
10	3	3	1	2	9
11	3	3	1	1	8
Mean	2.1	2.4	1	1.1	6.7

[a]Patient number is the same as the patient number in Table 2.

Magnetic resonance imaging scans were available for 9 of 11 patients at follow-up (Table 3). The MRI findings showed 50% to 100% defect fill in 6 patients (67%) and normal or

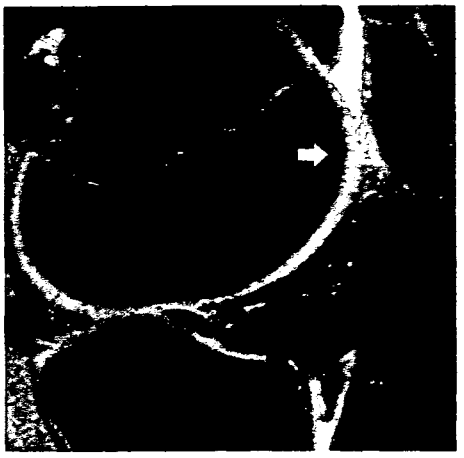

Figure 2. Sagittal MRI scan of patient 8 at 14 months postoperatively shows 50% to 100% defect fill with normal or nearly normal signals at the donor harvest site (white arrow).

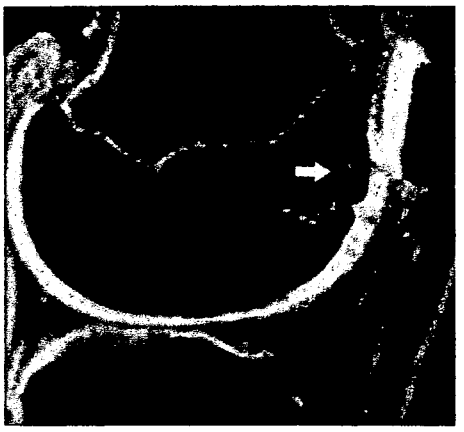

Figure 3. Sagittal MRI scan of patient 4 at 28 months postoperatively demonstrates 50% to 100% defect fill and large area of abnormal signals at the donor harvest site (white arrow).

nearly normal signals in 4 patients (44%) at the donor harvest sites (Figures 2 and 3). All patients except 1 showed no joint effusion. No subchondral bone marrow edema and hypertrophic changes at the donor sites were found in any patients. The overall MRI score was 6.7 points (range, 4-9 points).

DISCUSSION

In the standard technique of mosaicplasty, small cylindrical osteochondral grafts for cartilaginous lesions are harvested from a less weightbearing area of the knee joint, including the periphery of the lateral femur at the patellofemoral joint and the femoral intercondylar notch. Therefore, one of the most considerable limitations in performing this procedure is the adverse effect on donor sites. Especially in transplanting grafts from a normal knee into another joint, surgeons must prevent donor site complications. The current study showed that all patients except 1 achieved a maximum clinical and functional score of the donor knee at follow-up. In addition, all patients returned to their previous sport activities without any donor site disturbances. These results indicate no unfavorable effect of graft harvest on the donor knee in young athletes with capitellar OCD treated with mosaicplasty. To date, only a few authors[6,7,13,17] have reported donor site morbidity after mosaicplasty. Hangody et al[6] reported that the symptoms in the donor knee were resolved at 1 year in 98% of patients with a talar cartilaginous lesion. Although the current results agree with their data, their results were based on only clinical symptoms. To elucidate the effect of graft harvests on donor knees, subjective and objective assessments must be performed for patients with other joint lesions, such as the elbow or ankle joint. It is from this point of view that we emphasize the significance of our study. On the other hand, Reddy et al[17] indicated that osteochondral harvest from asymptomatic knees for the treatment of talar osteochondral lesions leads to a decline in knee function. Compared with their data, the age of patients and the size of osteochondral grafts in our study are younger and smaller, respectively. It is likely that these factors resulted in our favorable outcomes compared with those of Reddy et al.[17]

Regarding the intrinsic healing response at the osteochondral graft donor harvest site in mosaicplasty, a clinical report by Ahmad et al[1] showed that a donor site 8 mm in diameter at the intercondylar notch was filled with fibrous tissue with inferior material properties, compared with those of normal cartilage. Barber and Chow[4] arthroscopically demonstrated that the donor sites in the superior lateral intercondylar notch were covered with fibrocartilaginous scar tissue. The data obtained from a canine model also support these clinical results.[5] The current MRI evaluation suggested that 89% of donor sites had alteration in signal intensity, compared with that of adjacent cartilage. Henderson et al[9] stated that the MRI signal is a useful visual indicator of maturity of reparative cartilage, especially in comparison with the signal of adjacent normal articular cartilage. Based on these previous clinical and experimental results, the signal changes in our MRI evaluation indicate that the empty graft harvest sites are covered with fibrous or fibrocartilaginous tissue. In general, the edema of the underlying bone marrow indicates abnormal bone loading secondary to an immature cartilage cover.[9] In the current study, no subchondral bone edema was found in any donor sites. As mentioned above, osteochondral grafts were harvested from the superolateral periphery of the femoral condyle at the level of the patellofemoral joint. Simonian et al,[20] using cadaveric specimens, demonstrated significant contact pressure on this area. Our result regarding the bone edema suggests that no abnormal force distribution on the donor site may occur at follow-up. However, the significant contact pressure at the graft harvest sites covered with fibrous tissue might result in further degenerative changes or other problems in the donor knee. Long-term follow-up with a greater number of subjects after performing mosaicplasty will confirm this point.

An important technical consideration in harvesting osteochondral plugs is to prevent excessive bleeding from

the donor harvest sites. Bleeding in the early postoperative period seems to be a complication of such graft harvests. Hangody and Füles[7] reported that 34 of 652 patients treated with mosaicplasty had painful hemarthroses after surgery, and 4 of them resulted in further deep infections. In our cases, each donor tunnel was carefully packed with bone wax to prevent postoperative bleeding, and a drain was inserted. The mean total amount of bleeding from the knee joints was less than 20 mL, and effusion persisted for only a mean of 3 weeks postoperatively. We think that this manner can reduce apparent complications resulting from excessive bleeding from the donor sites.

There are some considerations in this study. First, the results were obtained from young patients with a mean age of 14 years. Second, the size of donor sites for graft harvest was relatively small. Third, the effects of bone wax on the cartilage regeneration process remain unclear. Although nonresorbable bone wax has been considered to inhibit osteogenesis,[2,16,24,25] no laboratory studies have clarified the effects of this material on cartilage repair. This reparative process is initiated by recruiting bone marrow stromal cells. Therefore, cartilage repair might be obstructed by packing a donor tunnel with bone wax. Further laboratory and clinical studies will be performed to elucidate this point. Finally, the minimum follow-up period of this study was relatively short. These factors might minimize the adverse effects of graft harvests on donor sites.

In conclusion, no adverse effects of osteochondral graft harvests on donor knee function were found after mosaicplasty for capitellar OCD in young athletes. On the other hand, MRI findings indicated that the empty site after harvesting osteochondral grafts was resurfaced with fibrous or fibrocartilaginous tissue. A careful assessment of the localization, size, and number of grafts for autologous osteochondral transfers must be made, along with long-term follow-up of these donor sites, to prevent the occurrence of donor site morbidity.

ACKNOWLEDGMENT

We thank Dr Jyunichi Ishikawa, Dr Takumi Kimura, Dr Kimitaka Fukuda, Dr Hisamitsu Ishikura, and Dr Tatsuya Masuko for the data acquisition.

REFERENCES

1. Ahmad CS, Guiney WB, Drinkwater CJ. Evaluation of donor site intrinsic healing response in autologous osteochondral grafting of the knee. *Arthroscopy*. 2002;18:95-98.
2. Alberius P, Klinge B, Sjogren S. Effects of bone wax on rabbit cranial bone lesions. *J Craniomaxillofac Surg*. 1987;15:63-67.
3. Anderson AF. Rating scales. In: Fu FH, Harner CD, Vince KG, eds. *Knee Surgery*. Baltimore, Md: Williams & Wilkins; 1994:275-296.
4. Barber FA, Chow JCY. Arthroscopic osteochondral transplantation: histologic results. *Arthroscopy*. 2001;17:832-835.
5. Feczkó P, Hangody L, Varga J, et al. Experimental results of donor site filling for autologous osteochondral mosaicplasty. *Arthroscopy*. 2003;19:755-761.
6. Hangody L, Feczkó P, Bartha L, Bodó G, Kish G. Mosaicplasty for the treatment of articular defects of the knee and ankle. *Clin Orthop Relat Res*. 2001;391:S328-S336.
7. Hangody L, Füles P. Autologous osteochondral mosaicplasty for the treatment of full-thickness defects of weight-bearing joints: ten years of experimental and clinical experience. *J Bone Joint Surg Am*. 2003;85:25-32.
8. Hangody L, Ráthonyi GK, Duska Z, Vásárhelyi G, Füles P, Módis L. Autologous osteochondral mosaicplasty: surgical technique. *J Bone Joint Surg Am*. 2004;86:65-72.
9. Henderson IJP, Tuy B, Connell D, Oakes B, Hettwer WH. Prospective clinical study of autologous chondrocyte implantation and correlation with MRI at three and 12 months. *J Bone Joint Surg Br*. 2003;85:1060-1066.
10. Iwasaki N, Kato H, Ishikawa J, Saitoh S, Minami A. Autologous osteochondral mosaicplasty for capitellar osteochondritis dissecans in teenaged patients. *Am J Sports Med*. 2006;34:1233-1239.
11. Kock NB, Van Susante JLC, Wymenga AB, Buma P. Histological evaluation of a mosaicplasty of the femoral condyle–retrieval specimens obtained after total knee arthroplasty: a case report. *Acta Orthop Scand*. 2004;75:505-508.
12. Kodama N, Honjo M, Maki J, Hukuda S. Osteochondritis dissecans of the talus treated with the mosaicplasty technique: a case report. *J Foot Ankle Surg*. 2004;43:195-198.
13. LaPrade RF, Botker JC. Donor-site morbidity after osteochondral autograft transfer procedures. *Arthroscopy*. 2004;20:e69-e73.
14. Marcacci M, Kon E, Zaffagnini S, et al. Multiple osteochondral arthroscopic grafting (mosaicplasty) for cartilage defects of the knee: prospective study results at 2-year follow-up. *Arthroscopy*. 2005;21:462-470.
15. Matsusue Y, Yamamuro T, Hiromichi H. Arthroscopic multiple osteochondral transplantation to the chondral defect in the knee associated with anterior cruciate ligament disruption. *Arthroscopy*. 1993;9:318-321.
16. Orgill DP, Ehret FW, Regan JF, Glowacki J, Mulliken JB. Polyethylene glycol/microfibrillar collagen composite as a new resorbable hemostatic bone wax. *J Biomed Mater Res*. 1998;39:358-363.
17. Reddy S, Pedowitz DI, Parekh SG, Sennett BJ, Okereke E. The morbidity associated with osteochondral harvest from asymptomatic knees for the treatment of osteochondral lesions of the talus. *Am J Sports Med*. 2007;35:80-85.
18. Roberts S, McCall IW, Darby AJ, et al. Autologous chondrocyte implantation for cartilage repair: monitoring its success by magnetic resonance imaging and histology. *Arthritis Res Ther*. 2002;5:R60-R73.
19. Shimada K, Yoshida T, Nakata K, Hamada K, Akita S. Reconstruction with an osteochondral autograft for advanced osteochondritis dissecans of the elbow. *Clin Orthop Relat Res*. 2005;435:140-147.
20. Simonian PT, Sussmann PS, Wickiewicz TL, Paletta GA, Warren RF. Contact pressure at osteochondral donor sites in the knee. *Am J Sports Med*. 1998;26:491-494.
21. Tegner Y, Lysholm J. Rating system in the evaluation of knee ligament injuries. *Clin Orthop Relat Res*. 1985;198:43-49.
22. Timmerman LA, Andrews JR. Arthroscopic treatment of posttraumatic elbow pain and stiffness. *Am J Sports Med*. 1994;22:230-235.
23. Tsuda E, Ishibashi Y, Sato H, Yamamoto Y, Toh S. Osteochondral autograft transplantation for osteochondritis dissecans of the capitellum in nonthrowing athletes. *Arthroscopy*. 2005;21:1270.
24. Wellisz T, Armstrong JK, Cambridge J, Fisher TC. Ostene, a new water-soluble bone hemostasis agent. *J Craniofac Surg*. 2006;17:420-425.
25. Wolter D, Mohr W, Kinzl L. Reaction of the bone and soft tissues to implanted bone wax in the sheep. *Chirurg*. 1975;46:459-462.

Chitosan-based hyaluronan hybrid polymer fibre scaffold for ligament and tendon tissue engineering

T Majima[1,2*], T Irie[1,2], N Sawaguchi[1,2], T Funakoshi[1,2], N Iwasaki[1,2], K Harada[3], A Minami[1,2], and S-I Nishimura[2,4]
[1]Department of Orthopaedic Surgery, Hokkaido University School of Medicine, Sapporo, Japan
[2]Frontier Research Center for Post-genomic Science and Technology, Hokkaido University, Sapporo, Japan
[3]Chemical Biology Institute, Sapporo, Japan
[4]Laboratory of Bio-Macromolecular Chemistry, Division of Biological Sciences, Graduate School of Science, Hokkaido University, Sapporo, Japan

The manuscript was received on 3 July 2006 and was accepted after revision for publication on 7 February 2007.

DOI: 10.1243/09544119JEIM203

Abstract: To establish medical use of tissue engineering technology for ligament and tendon injuries, a scaffold was developed which has sufficient ability for cell growth, cell differentiation, and mechanical properties. The scaffold made from chitosan and 0.1 per cent hyaluronic acid has adequate biodegradability and biocompatibility. An animal experiment showed that the scaffold has less toxicity and less inflammation induction. Furthermore, *in-vivo* animal experiments showed that the mechanical properties of the engineered ligament or tendon had the possibility to stabilize the joint. It was shown that newly developed hybrid-polymer fibre scaffold has feasibility for joint tissue engineering.

Keywords: chitosan, hyaluronan, scaffold, tissue engineering, ligament, tendon

1 INTRODUCTION

Severe ligament and tendon injuries are frequently treated with autograft reconstruction [1, 2]. On the other hand, the use of autograft will result in donor site morbidity. Tissue engineering is an emerging scientific approach that attempts to develop biological substitutes made from isolated cells and three-dimensional polymeric scaffolds [3]. The principal role of three-dimensional scaffolds in musculoskeletal tissue engineering is to provide a temporary template with the biomechanical characteristics of the native extracellular matrix (ECM) during the process of *in-vivo* tissue regeneration. Additionally, in living tissues, the authentic substrate for most cells is the ECM. The ECM adheres to cells via integrins, which are membrane-spanning heterodimeric receptors. Through cell–ECM adhesion, the ECM transduces physiological signals regulating cell growth, cell proliferation, cell differentiation, and matrix remodelling to the cells [4]. The ECM not only binds embedded cells together but also affects their survival, development, shape, polarity, and behaviour. Therefore, the ECM plays an important role in living tissue development and regeneration. For these reasons, it is believed that the ideal scaffold material should be one that mimics the natural environment in the ECM.

Some materials, including collagen gels, collagen sponges, and collagen constructs, have been used as scaffolds in ligament tissue engineering [5–9]. These materials, however, do not structurally mimic ligament-specific ECM. Furthermore, collagen fibre scaffolds suffer from batch-to-batch variability, making consistent reproduction of these constructs difficult [10]. The major limitation is that collagen scaffold has an immunogenic reaction [10]. Other scaffolds have limited applications, such as polyglycolic acid [8], because of its mechanical brittleness and the lack of functional groups for signalling molecules [11]. Consequently, in the living body, they do not provide sufficient mechanical support for the regenerated ligament or transduce mechanophysiological signals that significantly enhance ligament regeneration and remodelling processes to the embedded cells. Given the importance of glycosaminoglycans (GAGs) in stimulating various *in-vitro* tissue regenerative processes, the use of GAGs or GAG-like materials as components of a scaffold should be a reasonable approach for ligament tissue engineering.

* *Corresponding author: Department of Orthopaedic Surgery, Hokkaido University School of Medicine, N-15, W-7, Kita-Ku, Sapporo, 060-8638, Japan. email: tkmajima@med.hokudai.ac.jp*